THE PENNSYLVANIA STATE UNIVERSITY
SCHREYER HONORS COLLEGE

DEPARTMENT OF CHEMISTRY

Pressure-Induced Polymerization of UV Irradiated Benzoquinone Derivatives

ROBERT CONNOR BURNS
SPRING 2023

A thesis
submitted in partial fulfillment
of the requirements
for a baccalaureate degree
in Chemistry
with honors in Chemistry

Reviewed and approved* by the following:

Elizabeth Elacqua
Assistant Professor of Chemistry
Thesis Supervisor

Benjamin Lear
Associate Professor of Chemistry
Honors Adviser

Lori Stepan
Associate Teaching Professor
Faculty Reader

* Electronic approvals are on file.

ABSTRACT

Carbon nanothreads are the newest allotrope of carbon which involves carbon atoms that are sp^3 hybridized and in a 1-D order. These new molecules can be synthesized via a pressure-induced polymerization under uniaxial stress from a precursor containing sp^2 carbons in a ring. In this thesis, the report of the possible formation of nanothreads from a previously uncompressed molecule, benzoquinone, are shown. This molecule is nonaromatic and has favorable π-π stacking which bodes well for nanothread formation. In addition to this, the molecule has been exposed to UV light which has been shown to experimentally to help reduce reaction pressures for nanothreads. These compressions consistently result in a well-ordered solid that demonstrates the presence of sp^3 carbons. These results often take place at lower than expected reaction pressures for most nanothreads. In addition to benzoquinone, one of its derivatives, hydroquinone, as well as hydroquinone's structural isomers, resorcinol and catechol, have been compressed.

TABLE OF CONTENTS

LIST OF FIGURES

LIST OF TABLES

ACKNOWLEDGEMENTS

Firstly, I would like to thank Dr. Elizabeth Elacqua who excitedly asked me if I wanted to join her lab after trying to find someone to be my honors advisor. This proved to be one of the best decisions I made while at Penn State. She continued to be a positive person to be around and helped to motivate me with research and beginning my thesis.

I would also like to thank Margaret Gerthoffer who has been my amazing mentor for the past 2 years. She welcomed me very warmly into the Elacqua lab in the Fall of 2021 where we began a two month training process, so I could learn how to possibly make nanothreads. After two months of learning how shaky someone's hand is under a microscope while ruby picking, I finally got to compress my first sample and I fell in love with it. After this, she continued to support me with anything I need like running IR and XRD on my samples and encouraged me to stay the following summer to become immersed in the lab. Without her help, none of my research I conducted, or this thesis would be possible.

All of the Elacqua Lab has played a role in my development as a chemist. Most importantly, Morgan Murphy and Steve Huss. Whenever Margaret was running reactions upstairs or otherwise busy, these two were always there to help me. I always received constant support from both, and they were able to help me grasp what nanothreads are as well. Morgan, in particularly, made a large impact to me as she helped to support me and give me great encouragement especially when I was feeling like this was an impossible task. In addition to this she also gave me innumerable extra materials to me to help me understand why nanothreads are made and other supporting materials.

One last nanothread focused graduate student I would like to thank is Sikai from the Crespi and Terrones group. She helped show me other aspects of the lab and allowed me to take over her office space occasionally to make Raman figures.

My research would have been incomplete with Morgan Dierolf, a fellow undergraduate researcher. Her and I collaborated on many experiments together whenever the other could be there to monitor a compression.

Dr. Aaron Garner, my advisor, has allowed me to graduate on time and given me advice on what classes to take when as well as career advice which is invaluable.

Thank you to my honors thesis committee, Dr. Elizabeth Elacqua, Dr. Benjamin Lear, and Dr. Lori Stepan, for taking time out of your busy schedules to review the culmination of my undergraduate research in this thesis.

Additionally, the Benkovic Summer Research Award allowed me to conduct research over the summer of 2022 with partial funding. I am forever indebted for this as I would not have been able to complete my thesis without this additional time.

The Schreyer Honors College has also provided me with many scholarships and grants which have allowed me to focus more on my coursework than my job. Without this generous support I would not be the same student I am today.

Lastly, I'd like to thank all of my family and friends for their endless support and guidance that I have received throughout my life.

Chapter 1

Carbon Nanomaterials

1. Background of Carbon Nanomaterials

Researchers have long focused on the development of new carbon allotropes for a variety of purposes, including their tunable tensile strength and elastic modulus, as well as their high-performance ability to convert energy and energy storage.[1-2] The small size of these materials presents many dynamic options for their utilization. The ever-increasing rate for energy in the technological era has demanded for an increase in technology possessing such powers. This has increased carbon nanomaterial research ever since carbon nanotubes were first discovered in the early 90's.[3]

Carbon is a well-known element to form many different solid-state allotropes, all of which bear different properties as dependent on their dimensionality and hybridizations. In particular, the low dimensional allotropes such as fullerenes, diamondoids, nanotubes, and graphene have drawn much of this attention due to properties that are described above as they exhibit these properties better.[4] Some examples can be found in Figure 1.1 shows major examples of the different carbon allotropes discovered ordered by hybridization and dimensionality. These molecules have been discovered gradually and have involved a variety of techniques such as chemical vapor deposition, isolation from natural materials, and arc discharge to synthesize these materials. Carbon networks are largely insoluble with organic solvents, meaning the traditional use of solvents within chemistry cannot be used. As a result, synthesis in the solid-state provides a method of synthesis without solvents with controlled reactivity to restrict explicit carbon bond formation of a given dimension and hybridization.[5] High pressure

methods have also been shown to reduce the reaction barrier in addition reactions that are experiencing a negative volume change.[6] This property will become crucial later for the formation of some carbon allotrope varieties. Experimentation had yielded allotropes of carbon of all dimensions and hybridizations, except for the 1-D sp^3 carbon allotrope that wasn't discovered until 2015.[7] This newest allotrope was named carbon nanothreads as they formed a very long and ordered thread like structure. They were discovered from the high pressure compression of benzene. Benzene has been previously compressed and yielded only amorphous products, but upon slowing down the reaction rate greatly to allow for kinetic control permits for nanothreads to be made from benzene.[7,8,9,10]

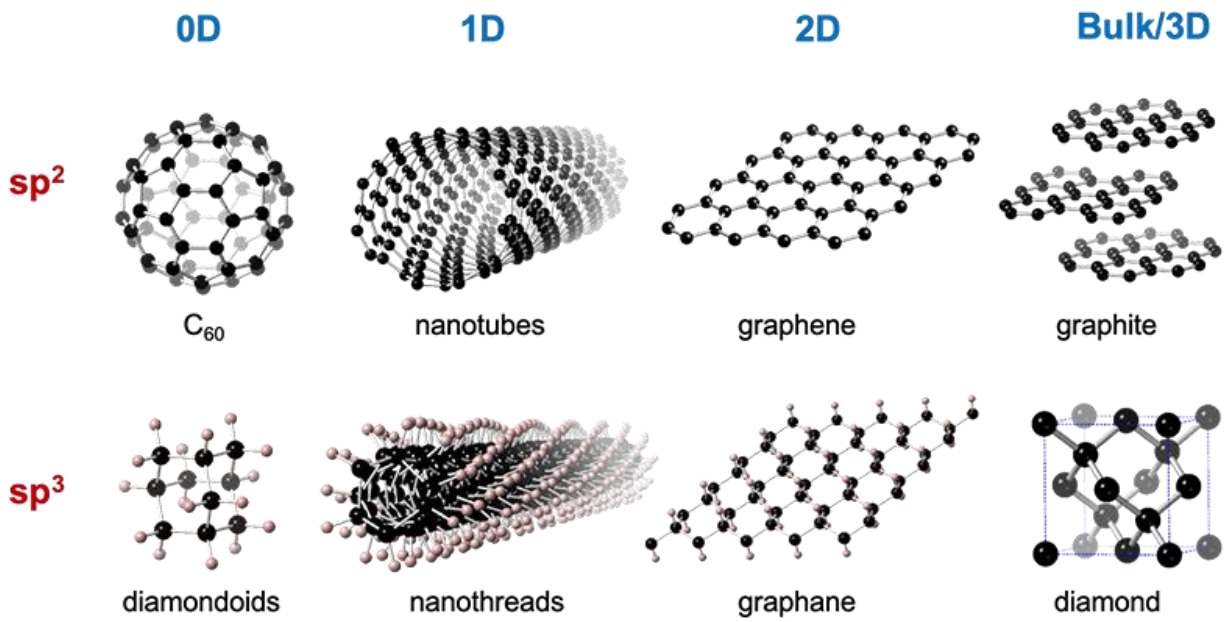

Figure 1.1. Different carbon allotropes in different hybridizations and dimensions.

2. Carbon Nanothreads

In 1979, Arthur C. Clark published the science fiction book *The Fountains of Paradise* where he illustrated revolutionary space elevators that were hoisted by threads of diamond.[11]

These threads became known as nanothreads and were predicted theoretically in 2001 and 2011.[12,13] In 2015, Fitzgibbons *et. al.* were able to successfully compress benzene and recover at atmospheric pressure a crystalline, one-dimensional, sp^3-hybridized solid known as carbon nanothreads.[7] This discovery was accidental in nature, but makes sense as benzene has a favorable crystal structure which allows nanothread formation. In the high pressure phase solved around 1.5 GPa (Figure 1.2), stacks of benzene molecules illustrate close contact distances through π-π stacking. However, as illustrated, multiple stacks of benzene exist in the structure, illustrating the necessity of slow compression to select a pathway set closest to the applied stress. Theorists have recently predicted that these nanothread bundles have a high tensile strength and high mechanical energy storage to one day out-pace lithium-ion batteries with three times the energy storage capabilities.[7,14] Carbon nanothreads are also distinct from many other synthetic carbon nanomaterials in that it can form nearly single crystals on a macroscopic scale where most other nanomaterials cannot.[15]

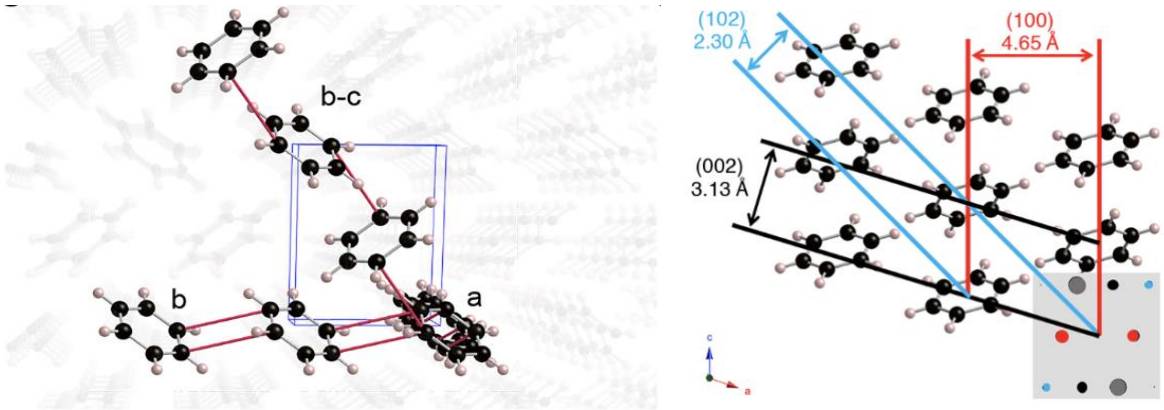

Figure 1.2. Different unit cell axes (blue) and polymerization pathways (red) of phase II benzene (left). Benzene crystal structure from B-axis with diffraction planes and interplanar spacings at 23 GPa (right). Reprinted with permission from *J. Am. Chem. Soc*, 2017, *139* (45), 16343–16349.

The discovery of this new carbon allotrope brought questions of how the mechanism to their formation works. These nanothreads can form a variety of bonds to create themselves and it was theorized they undergo multiple polymerizations to form the final polytwistane-like structure as this is the lowest energy for nanothreads.[16] In addition to this nanothreads can form 2, 4, or 6-fold structures which is dependent on the number of bonds that get formed to adjacent molecules. They are most commonly 6-fold as this is the most saturated version of nanothreads, but if they are not fully saturated 2 or 4-fold varieties are represented.[17] This phenomenon occurs due to the nanothreads not being pure. They can have multiple defects, but they are resistant to them so the structure can continue.[15] Nanothreads are believed to form via a [4+2] Diels-Alder cycloaddition that can occur thanks to the collapse of π-π stacking. The cycloaddition forms an olefinic backbone that undergoes a cascading [2+2] cycloaddition to zipper the molecule into the fully saturated nanothread backbone.[17] The resulting structure can be observed in Figure 1.3. Over the years of compressing carbon compounds at high pressures, no one had attempted a kinetically controlled experiment in which the compound was slowly compressed to 23 GPa at room temperature as shown in Figure 1.3. Prior to this compression, carbon has only formed disordered amorphous carbon networks under pressure.[8,9,10] Through further experimentation in 2017, single nanothread crystals were found to form only under uniaxial pressure from molecules, such as benzene, that typically do not polymerize through topochemical pathways.[15]

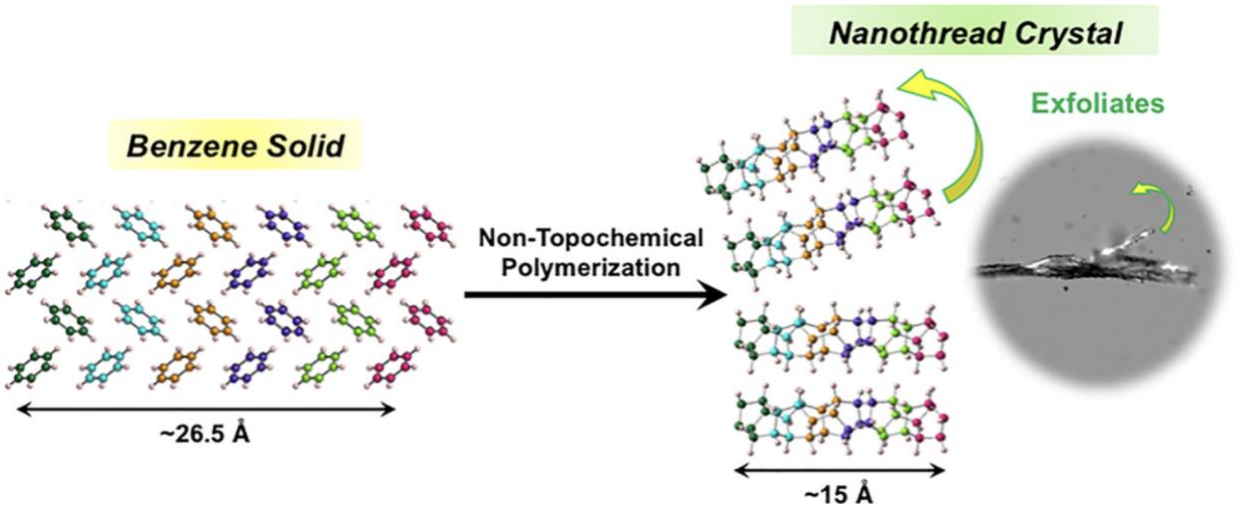

Figure 1.3. Carbon nanothread formation at 23 GPa and 300 K showing reduction in distance of benzene. Nanothread fibers also shown. Reprinted with permission from J. Am. Chem. Soc, 2017, 139 (45), 16343–16349.

These major discoveries left researchers wondering if other simple aromatics could form nanothreads. In 2018, pyridine-derived nanothreads were first discovered, illustrating that nanothread synthesis can be diverse from different crystal arrangements, aromatic properties, and heteroatoms.[18] Research also found that molecules such as thiophene, cubane, and furan all formed nanothreads.[19,20,21] Each nanothread discovery reveals something profound about them which enables for control of different properties or synthesis. For example, thiophene compression shows that orientational order can be achieved as derived from the precursor crystal structure and compressing furan illustrates a remarkably lower reaction pressure (15 GPa) due to the tuned reduced aromaticity.[19,21]

Co-crystals of naphthalene and octofluronaphthalene were compressed in 2019 to reveal that the alternating polarities of these molecules causes favorable π-π stacking which can enable nanothread formation.[22] Following this discovery of utilizing co-crystals, others were compressed, but not all resulted in successful nanothreads such as benzene:hexaflurobenzene

which results in graphane.[23] In combination with an idea from a 2020 paper showing that careful precursor selection can result in functionalized nanothreads,[24] phenol:pentaflurophenol crystals were compressed to reveal they react by following a keto-enol tautomerization to initiate the nanothread.[25]

One additional paper discusses the potential of using co-crystals to form nanothreads. This relies upon electronics within the nanothread as co-crystals can cause ordering within the stacks. This is accomplished by having two molecules, one that has electron donating groups attached to it and another with electron withdrawing groups attached. This causes an alternating stacking of electron-rich to electron-poor aryl rings, leading to the formation of sequence-defined nanothreads.[26]

Upon initial discovery of nanothreads, it was theorized that their reaction pressures could potentially be reduced by thermal and photochemical means. Our group recently reported that both pyridine and furan can independently form nanothreads at a reduced pressure when exposed to UV irradiation in a Diamond Anvil Cell (DAC) using a 16 mW Hg lamp. These molecules have been compressed previously reacting at 23 and 15 GPa, respectively.[18,21] Furan has reduced pressure activity compared to benzene due to its reduced aromaticity respective to benzene. The addition of UV light resulted in a reduced reaction pressure of 1.4-fold for pyridine and 1.9-fold for furan. These findings indicate that photochemical means can lower. In addition to these experimental findings the team also found UV exposure may have altered the reaction pathway for the compression of furan. Photochemically, it became more favorable to initiate nanothread formation though a [4+4] cycloaddition followed by a series of [4+2] cycloadditions pathway, rather than a whole series of [4+2] cycloadditions reactions.[17] As a result, both chemical precursor design (through reducing aromaticity and forming co-crystalline stacks) in addition to

external photochemical irradiation are possible methods to reduce the necessary pressure to form nanothreads, helping to guide future research into scalable opportunities.[27]

3. High-Pressure Solid-State Chemistry

Solid-state chemistry is generally hard to carry out as a reaction can only occur where adjacent molecules are in direct contact with one another, so different chemical pathways must be utilized as well. High-pressure solid-state chemistry has long been believed to cause pressure induced polymerizations for carbon networks. Pressure will convert unsaturated molecules into saturated molecules as the thermodynamic driving source can become extremely large with pressure being the main thermodynamic variable.[28] Saturated molecules are favored under pressure as they occupy a smaller space than unsaturated networks.[28]

Most experimentation from the compression of benzene to 10s of GPa has largely only yielded amorphous products.[28] Many different pathways can form polymers in the solid state resulting in these amorphous compounds. To form a crystalline product, excess reaction pathways must be disfavored or desired pathways must be favored via different constraints. These constraints include explicit crystal design, where sterics and electronics can both alter the closest contact distance in a molecular system. In addition, altering the kinetics of the reaction, where temperature or pressure rate can be altered can change the high-pressure phases and the dynamics of crystal collapse by inducing reactions such as cycloadditions in the case of carbon nanothreads.

There are many devices to that can be used to carry out high-pressure experiments. Some of the most widely used high-pressure devices are the DAC, two opposed diamonds glued to a metal seat and put together via screws, and the Paris-Edinburg press (PE press), a device in

which a filled gasket is squeezed from all sides from two anvils encapsulating the gasket. Each device has its own distinct advantages and disadvantages. The DAC can reach over 500 GPa in pressure, but it results in a small sample on the nanogram scale due to the small surface area of the diamond tips (culets). However, the small surface is the way a DAC can achieve such high pressures via $P = F/A$. This device works by applying pressure on a sample smashed between two diamond culets as contained in a stainless steel gasket. The diameter of each diamond culet has a small surface area of only a few hundred microns (10^{-6} m) wide. The culets may also be cut to be flat or beveled in order to generate larger pressures.[29]A schematic of a DAC can be found in Figure 1.4.

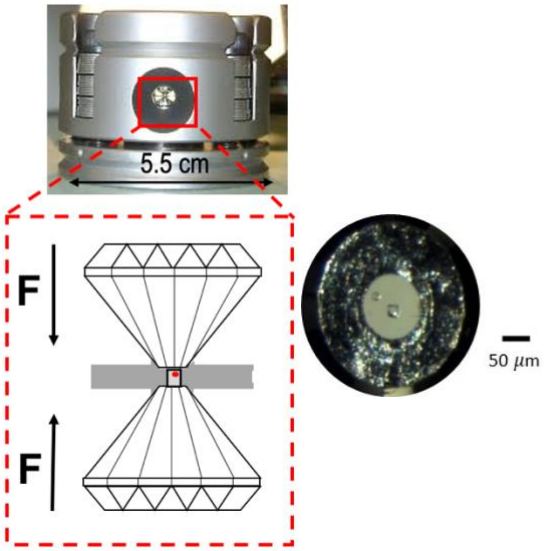

Figure 1.4. Image of a Diamond Anvil Cell (top left), schematic diagram of a DAC (bottom left) and a sample view of a DAC under microscope containing a ruby (right).

Within the center of a DAC sits the sample being compressed. To properly load a sample, it must be contained within a metal gasket. Designed for the purposes of compressing primarily soft organic materials, the gasket is composed of hard T301 stainless steel to avoid both

reactivity with the substrate and adhesion to the diamond. Each gasket is made specifically to each pair of carefully aligned diamonds. This gasket is first indented into the opposed diamond tips to mold into the shape of the diamond anvils to create a cavity for loading. Following indentation, the sample chamber is formed by drilling a hole into the pre-indented gasket around ¼ to ½ the diameter of the culet. This gasket will not only serve as the sample chamber, but also to seal the sample from ambient conditions. To measure the pressure achieved within the sample, a ruby chip must also be placed within the gasket as a known pressure standard to measure its fluorescence in correlation with applied pressure. The ruby chip is clear and its shifting under pressure has been calculated into an equation available to the public.[30] The ruby fluoresces around 694.22 nm at ambient conditions and will red shift as it continues to climb in pressure.[29]

DACs have a unique advantage for light transmission due to the diamond's ability to allow light to pass through it. This is particularly advantageous when trying to complete ultraviolet (UV) light experiments. The ability to transmit light in other high-pressure devices is hard to come by. One other way to alter reactions within a DAC is to increase temperature. Due to the small nature of a DAC, it can be heated in a controlled and isolated environment easily.[29]

One other distinct advantage of DACs is the ability to conduct *in situ* characterization using the same advantage of diamonds described above. At Penn State, the primary characterization *in situ* method to study nanothread formation is Raman spectroscopy, which measures the vibrational modes within the molecule from polarizability. Raman spectroscopy is non-destructive if the laser intensity is not too high to burn carbon-based samples. IR spectroscopy also can be collected *in situ* and instead measures different active modes as dependent on the dipole moment of bonds. X-ray diffraction (XRD) is another common *in situ* measurement that can be collected, but the X-ray source must be high flux as collected from

synchrotron radiation. Carbon materials have a low atomic number and the beam must be focused on a 5-micron sample between the two opposing diamonds.[29]

After recovery of a sample, nanothread samples can also be analyzed via XRD, IR, and X-ray Photoelectron Spectroscopy (XPS) studies. The former two rely on the same techniques described above. XPS can help identify the chemical composition of a sample by utilizing the photoelectric effect and the energy of photons coming off a surface. All these techniques are combined with theoretical studies to confirm the identity of nanothreads in particular.

PE presses can be utilized for *in situ* characterization techniques relying on visible light, but typically do not as most utilize polycrystalline diamonds that are not visibly transparent. However, for larger scale syntheses, PE cells can generate larger sample volumes on the scale of milligrams. Due to their larger volume, PE presses max out in pressure around 28 GPa compared to over 500 GPa for a DAC. They are also compatible with some of *in situ* characterization techniques like neutron diffraction but lack the ability for laser experimentation to be completed *in situ*. These advantages make PE presses better suited for when the reaction pressure is known and when trying to achieve a larger sample for external characterizations. Figure 1.5 shows a schematic for a PE cell.[29]

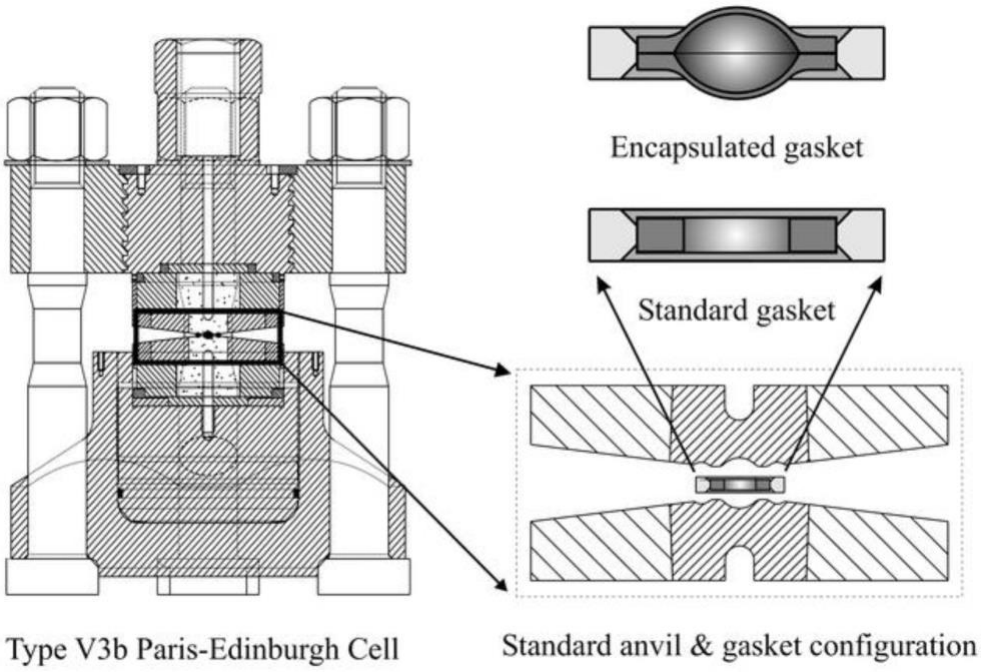

Figure 1.5. Schematic diagram of a type V3b Paris Edinburgh Press and accompanying gaskets. Reprinted with permission from J. Appl. Cryst. 2002, 35, 122–125.

4. Benzoquinone and Hydroquinone as Potential Precursors for Nanothread Formation

In expanding the possible diversity of nanothreads that could be formed at a reduced pressure, the compression of molecules that may be explicitly triggered by UV light may lead to a probable candidate that forms at reduced pressure. One such molecule that could possibly be viable is benzoquinone, a molecule with a six-fold carbon diene ring containing diones substituted *para* from each other (Fig. 1.6). The molecule's crystal structure is moreover beneficial as there are closely eclipsed stacks already ideal for nanothread formation. As discussed previously, a molecule must have closely eclipsed aryl rings to react at a critical threshold of 2.6 Å, which is observed in benzoquinone with a centroid:centroid distance of 4.8 Å at ambient pressure.[31] The benzoquinone molecules are slip-stacked as observed in the right

image of Figure 1.7. When viewed down the *b*-*c* axis shown in the left image of Figure 1.7, the molecules are eclipsed, illustrating the hypothesized thread-forming axis.

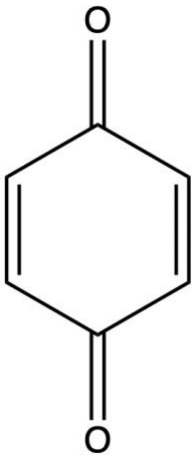

Figure 1.6. Benzoquinone molecular structure

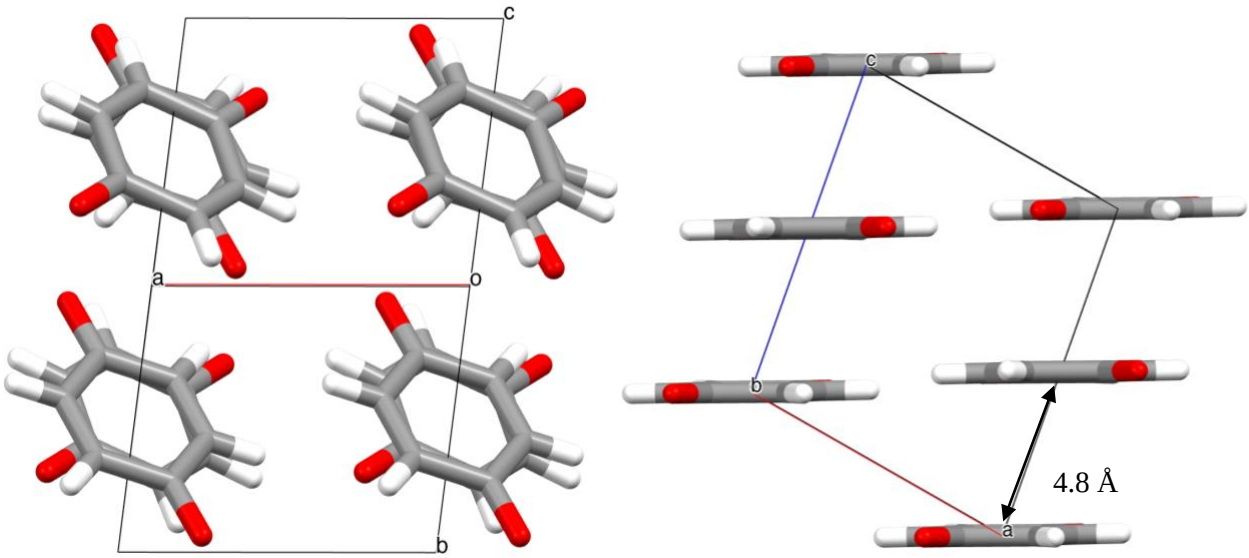

Figure 1.7. Benzoquinone crystal structure viewed from the b-c axis (left) and the b axis (right).

In previous studies, benzoquinone is non-aromatic, which bodes well for lending a hypothesis for a reduced reaction pressure as hypothesized with prior studies of furan.[15] This makes sense as it does not follow Huckel's rule of 4n+2.[32] Moreover, under UV light, benzoquinone can isomerize into hydroquinone.[33] Benzoquinone at ambient pressure will

transform into an intermediate radical semiquinone and eventually undergo a complete transition to hydroquinone as described in Figure 1.8.

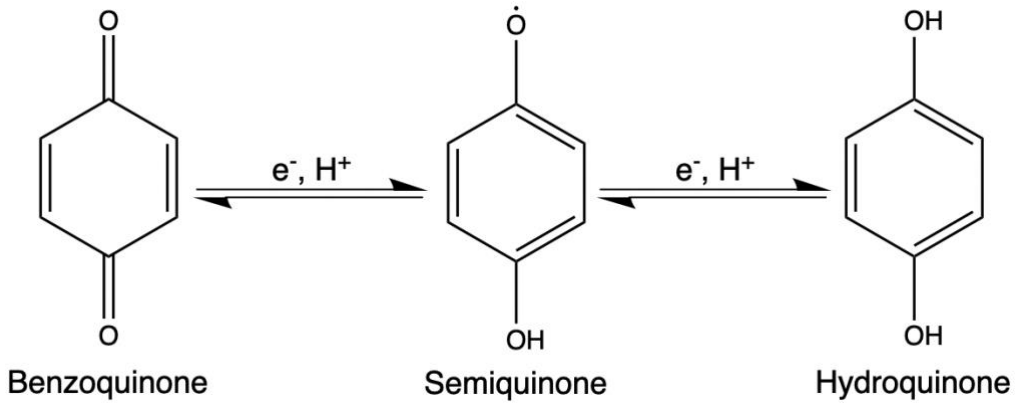

Figure 1.8. Isomerization of benzoquinone into hydroquinone.

This isomerization has multiple benefits that could potentially make nanothreads more scalable. The benzoquinone molecule make require a lower reaction pressure or even become a nanothread when compressed while simultaneously exposed to UV light.[27] While under pressure, this molecule could potentially isomerize to hydroquinone to form threads containing multiple -OH groups off the backbone. While undergoing an isomerization, the benzoquinone and hydroquinone molecules could form a base unit which could serve to lower the reaction energy for the propagation of nanothreads. This initiating base unit would be like that of co-crystals[25,26] When in a co-crystal, these molecules could make ordered stacks, and hydrogen bonding could occur between benzoquinone and hydroquinone.

Hydroquinone could also be a potential nanothread precursor, but it lacks some of the characteristics found in benzoquinone that prove beneficial to nanothread scalability. The crystal structure for hydroquinone shows it may be beneficial for nanothread formation, but it does not form stacks of adjacent aryl rings as compared to the benzoquinone as observed in Figure 1.9. The centroid:centroid distance is 5.4 Å, about 0.6 Å longer than benzoquinone. Hydroquinone is

aromatic, albeit less aromatic than other molecules that have been compressed before, unlike benzoquinone.[34] The crystal structure of hydroquinone is primarily affected by hydrogen bonding as observed in the right image of Figure 1.9. This could prove to be beneficial to help with preventing the crosslinking reactions that are present in many amorphous materials and instead direct polymerization to form nanothreads.

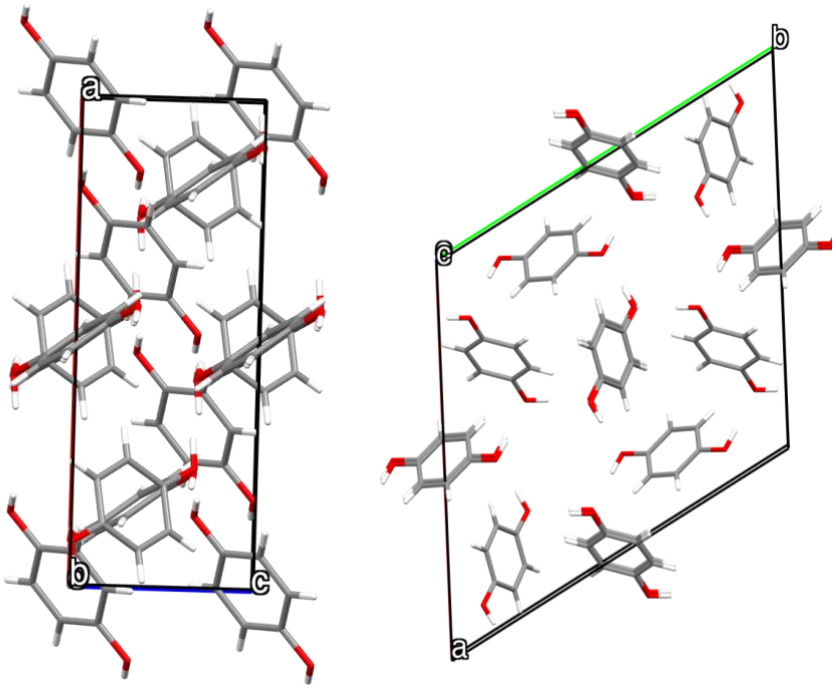

Figure 1.9. Crystal structure of hydroquinone down b-axis (left) and down c-axis (right).

There are additional benzoquinone derivatives, catechol and resorcinol, which are very similar to hydroquinone, but have alcohol groups ortho and meta to one another, respectively, as shown in Figure 1.10. The crystal structure of catechol and resorcinol are modeled below in Figures 1.11 and 1.12, respectively. The crystal structure of catechol is much more favorable to nanothread formation with a smaller centroid:centroid distance of 4.6 Å, but the stacking of neighboring molecules is opposite the direction of each other causing there to not be one single axis of reaction. This will make it tougher to form nanothreads from catechol. Resorcinol's crystal

structure is the least favorable to nanothreads as it is slipped across each other and has a farther centroid:centroid distance of 5.2 Å. Both molecules possess an axis down which they can react making them at least somewhat viable, but not as much as hydroquinone or benzoquinone.

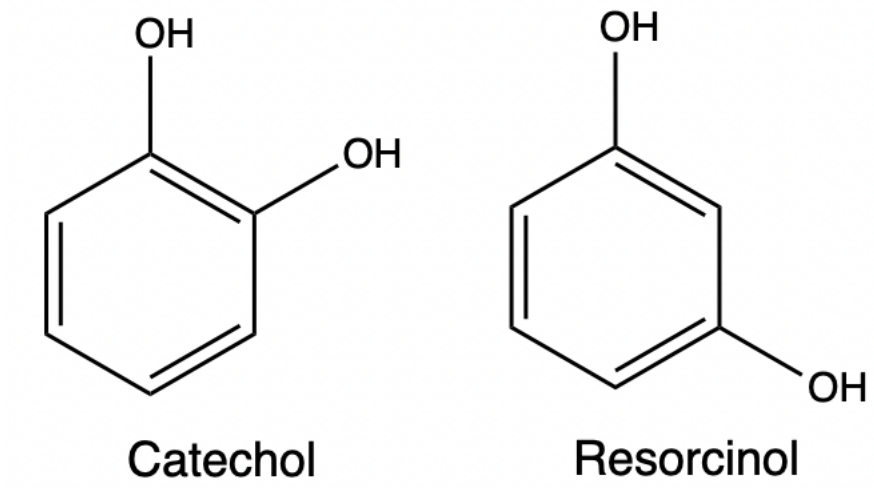

Figure 1.10. Molecular structure of catechol (left) and resorcinol (right)

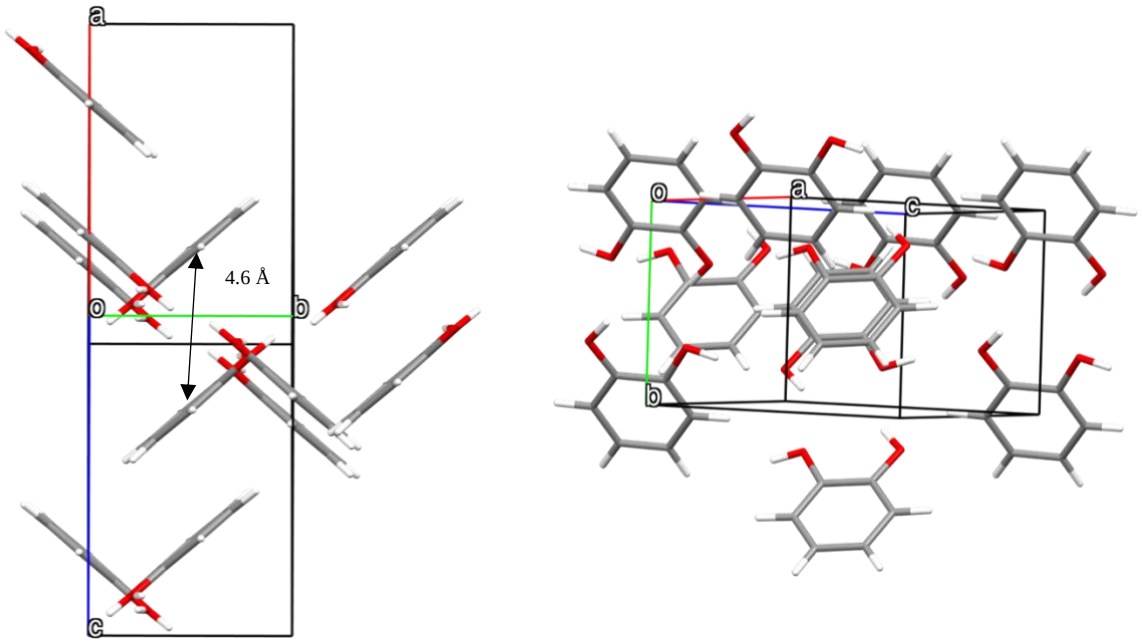

Figure 1.11. Crystal structure for catechol down a-c axis (left) and down a possible axis of reaction (right)

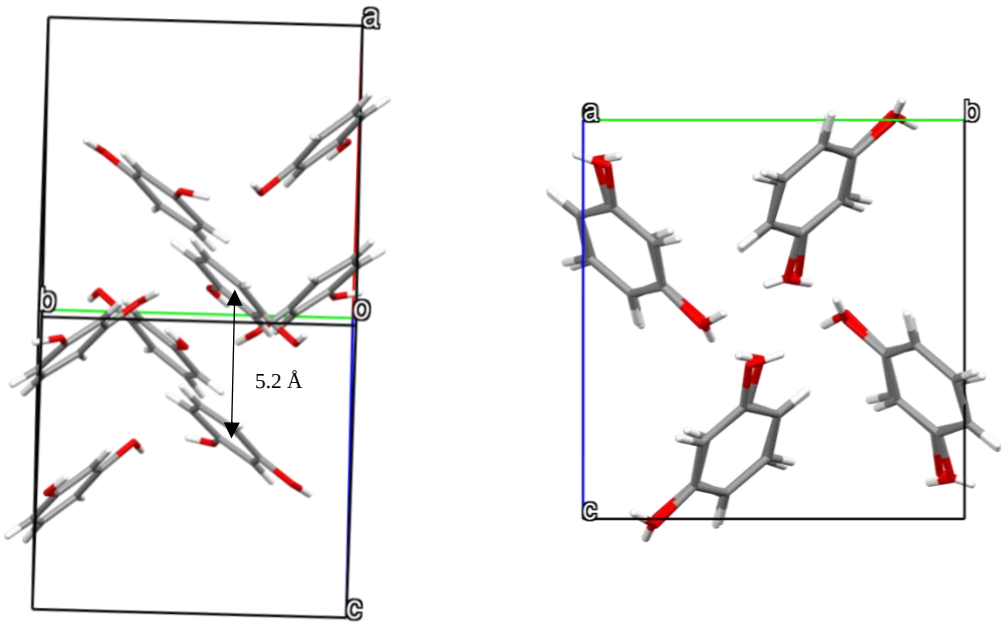

Figure 1.12. Crystal structure of resorcinol down a-c axis (left) and a-axis (right)

Benzoquinone and hydroquinone both are hypothesized to produce nanothreads from their reduced aromaticity to their favorable stacking patterns, but benzoquinone possesses the distinct advantage of isomerizing under UV light. This transformation makes it possible to become hydroquinone or resist this transition when under pressure. The unique properties of benzoquinone may help it to make nanothreads at lower pressures than many other molecules (less than 23 GPa). The high-pressure behavior of these molecules will thus be explored in the remaining chapter of this thesis to provide insight in future nanothread design.

Chapter 2

Compressions of Benzoquinone

1. Benzoquinone Viability for Nanothread Formation

Out of all the related compounds benzoquinone is hypothesized to require a reduced reaction pressure to become nanothreads compared to benzene. This hypothesis has a few justifications ranging from the compound being nonaromatic to the heteroatoms being present both of which aid in nanothread formation and in reduction of reaction pressures. The isomerization of benzoquinone into hydroquinone could also act as an initiator or the UV light under pressure could be an initiator as well. This allows for lower reaction pressures as illustrated previously with furan and pyridine derived nanothreads. UV light might already be the initiator in hydroquinone's compression. Above all, benzoquinone has a very friendly crystal structure to form nanothreads with a nearly eclipsed stacking pattern as well as a short centroid:centroid distance of 4.8 Å. Together these qualities mean that benzoquinone may be a likely nanothread-forming molecule that possesses other unique advantages not previously studied in other nanothreads.

Benzoquinone when compressed could undergo many pathways when exposed to UV light under high-pressure. Hopefully the molecule will become excited and propagate via [2+2] cycloadditions to form nanothreads. If this does not happen, there is likely an isomerization happening. The isomerization could happen throughout the entire molecule without any polymerization into nanothreads. A third scenario could involve the reactant partially

isomerizing into hydroquinone while simultaneously polymerizing to form nanothreads with defects along the axis of reaction.

As detailed below, benzoquinone will be compressed in a complete array of methods such as fast non-UV & UV compressions and slow non-UV and UV compressions. These experiments will help to identify an isomerization between hydroquinone and benzoquinone or nanothread formation with UV light and allow us to see what happens when there is no UV light present. Likewise, nanothreads have been previously shown to react differently under kinetically controlled reactions versus fast compressions, so the reaction could begin at different points.[7] The unique advantages of benzoquinone discussed above may help it to make nanothreads at lower pressures than many other molecules and allow one to see transitions to hydroquinone under pressure.

2. Fast Benzoquinone Compressions

Experimental Summary

A T301 stainless steel gasket was indented to approximately 12 GPa which achieved a width of 45-55 μm. After this an 80-100 μm hole was drilled with an electric discharge machine, and the gasket was placed into a symmetric Diamond Anvil Cell (DAC) equipped with 400 μm culet Type II diamonds. One ruby chip was placed at the center of the culet of both the upper and lower diamonds to act as a pressure standard.[1] Benzoquinone was loaded into the gasket as a powder. It was loaded until there was no light passing through. The sample was hand tightened to ~3 GPa to ensure a seal. Raman spectroscopy data was taken before further compression. The DAC was compressed at a rate of ~9 GPa/hour stepwise with Raman data taken in between until

maximum photoluminescence (PL) was obtained via Raman. Upon reaching maximum pressure, the DAC was rapidly decompressed to half the maximum pressure and at 1-2 GPa with an associated Raman data set.

A Renishaw inVia Raman spectrometer and microscope was used with a laser power of 1.34 mW and a 633 nm laser for *in situ* scans. To remove excess light a 5 μm pinhole was used. To get the laser to focus on samples through the diamonds, a long-pass 20x objective of 0.35 NA was used. If UV radiation was used, then it was projected through the top of this microscope with an output power of 96 mW, found using a Coherent PM3Q thermophile power sensor. The predicted power directed towards the sample is approximately 16 mW.[27]

Synchrotron radiation was used for XRD at the Advanced Photon Source (APS) at Argonne National Laboratory on the recovered sample. The 16-BM-D beamline created a 30 keV 5x5 μm beam with the MAR345 detector. The recovered sample has wide-angle reflections of ±32° ω-scans with 10s/deg. of exposure in a 75 μm square area over three regions of the sample. The Dioptas software interpreted the resulting images to account for any shadows or absorptions of the diamond.[35]

IR data was obtained using a Bruker Hyperion 3000 Microscope. This resulted in a diffraction limited spatial resolution of three 10 μm spots in each gasket for samples in the gasket. After focusing on a sample, transmission spectra images were found with an MCT detector. The sample has ATR spectroscopy performed on it using a FTIR Bruker Vertex V70 possessing an ATR attachment sampling accessory.

Non-UV Results

To properly determine benzoquinone's potential, a fast compression of benzoquinone must be done to determine when max PL is reached. This happens when all peaks have

dissipated to the point where their signals cannot be seen (usually the Raman spectrum will become wavy at this point). On a molecular scale this means that the rate of fluorescence emission, which Raman spectroscopy captures, is lower than that of PL emissions. This compression resulted in finding that PL stopped increasing at 16 GPa. The Raman spectrum can be found below in Figure 2.1. The large peak around 1400 cm^{-1} at 1.09 GPa is associated with the ruby standard and can be ignored. The peak at approximately 1660 cm^{-1} is present due to the C=O stretches. PL begins in this figure around 6.90 GPa, where a reduction in peak intensity can also be observed. Between these points are also a disappearance of the lattice modes found below 400 cm^{-1}. A peak table can be found in Table 2.1. Presumably this means that the crystalline benzoquinone has either begun a phase change into an amorphous compound since there are no other lattice present or PL has begun to overshadow them. The peak representing the C=C bonds within the ring also shifts left when increasing the pressure, meaning that they are lower in energy when they are closer to one another. As pressure increases, peaks should shift to the right, but peaks shifting to the left indicate a reduction in energy. These shifts happen due to the change in bond length, so peaks should shift right under pressure due to reduced bond lengths and because the bonds are getting closer to one another.[2]

IR spectroscopy of the recovered sample revealed that it was too oversaturated to get an accurate measurement. This was caused by a small drill hole where the light from the IR was reflected to the detector much more intensely than the sample, so in the future larger samples should be made. The sample was also analyzed via synchrotron XRD where an extremely weak ring can be observed at 5.3 Å. This analysis revealed the solid compound was indeed crystalline indicating that a fast compression of benzoquinone does result in a crystalline solid; it could be a nanothread.

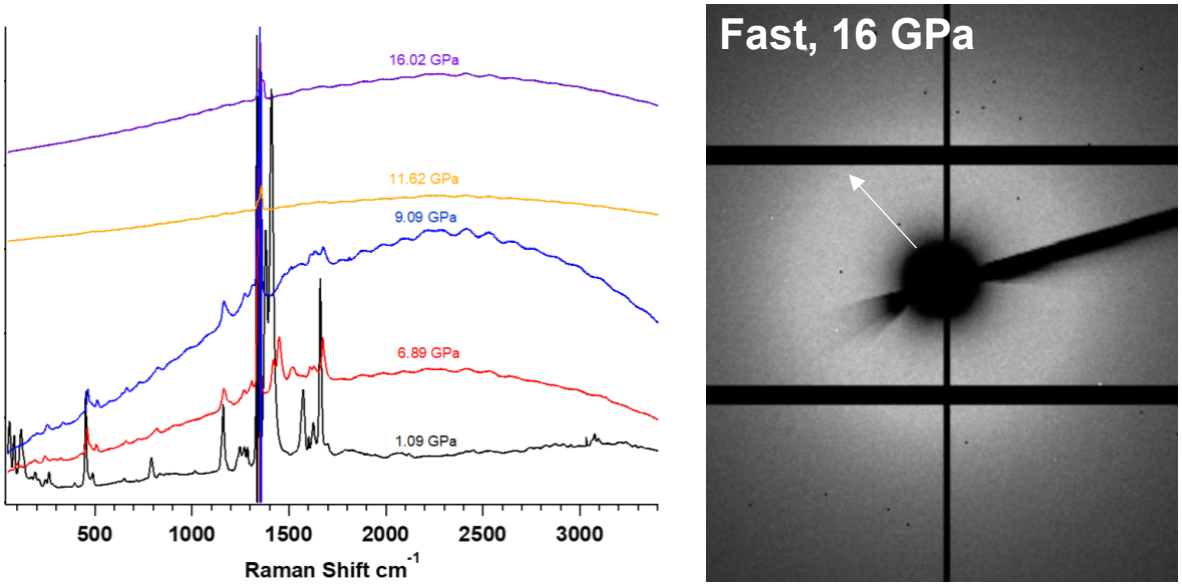

Figure 2.1. In situ Raman spectra (right) and XRD image (left) of the recovered sample for fast compression to 16 GPa with a d-spacing of 5.3 Å

Table 2.1. Peak assignment table for 16 GPa fast compression of benzoquinone.

Peak Assignments	Literature (cm^{-1})[36]	Experimental (cm^{-1})
C-H sp^2	3044, 3062	3050, 3075, 3095
C=O Stretching	1686	1661
C=C Aromatic	1667	1572, 1603, 1626
Diamond	-	1350
C-H bend	745, 1236	791, 1247, 1270, 1287
C=C	1000	1016
Ring Breathing	443, 770	453, 490

Fast UV Compressions

Knowing that benzoquinone may form nanothreads during fast non-UV compressions, it was studied under a fast UV compression. The exposure to UV light may allow for the

isomerization to hydroquinone and initiate the pressure-induced polymerization. This compression went up to 10 GPa while it was being exposed to UV light hourly with similar stepwise increases in pressure. This resulted in an accumulation of 4 hours of UV exposure over the entire compression. The Raman data for this showed nothing new compared to Figure 2.1. However, the sample yielded much more promising results in IR and XRD analysis than the previous experiment. When IR data was taken of the sample a massive reduction in sp^2 character and an increase in sp^3 character was observed as shown in Figure 2.3. Meanwhile XRD data revealed an intense diffraction ring and many other scattering patterns (which are likely small crystalline molecules). Once this sample was washed, a weak diffraction ring was observed, which is likely to be something new.

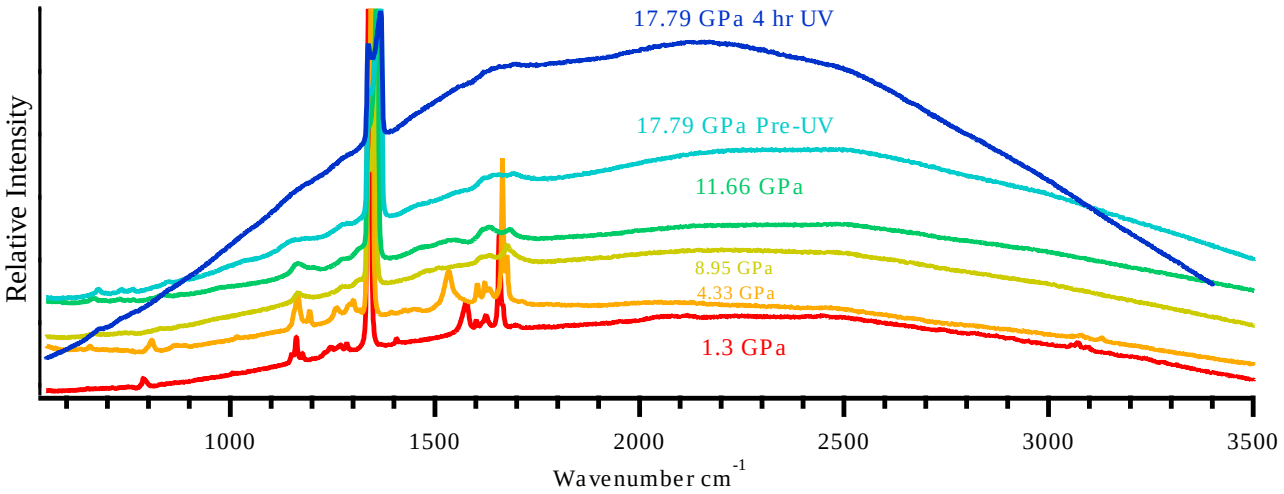

Figure 2.2. Raman spectrum for 18 GPa fast UV compression

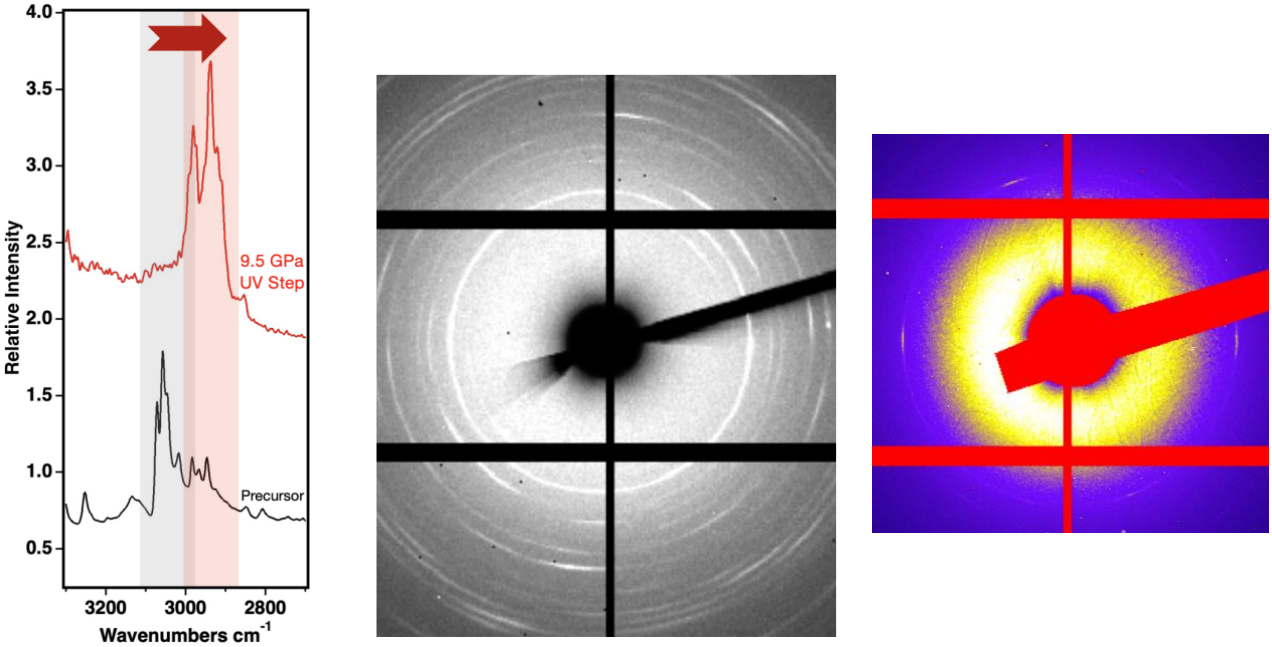

Figure 2.3. IR spectroscopy of benzoquinone (black) and recovered sample (red) (left), recovered XRD sample (middle), and washed XRD sample with small molecules washed away with a d-spacing of 5.2 Å (right).

Further experimentation was completed by compressing benzoquinone to ~18 GPa and exposing to UV in order to see if additional nanothreads could be made with elimination of any small molecules present. This could determine whether a higher pressure is needed to recover nanothreads without recovering other small molecules. Preliminary results of Raman data did not show anything profound as shown in Figure 2.2. No other analysis techniques were performed on this sample due to time constraints.

These results could possibly be indicative of nanothread formation, but further analysis would likely be needed such as XPS and theoretical studies to help back up the confirmation of this claim. There should also be more experimentation with the fast UV method. This could reveal when reaction pressure occurs and when all precursor is used up.

3. Slow Non-UV Benzoquinone Compressions

Experimental Summary

A T301 stainless steel gasket was indented to approximately 12 GPa which achieved a width of 45-55 μm. After this an 80-167 μm hole was drilled with an electric discharge machine, and the gasket was placed into a symmetric Diamond Anvil Cell (DAC) equipped with 400 μm culet Type II diamonds. One ruby chip was placed at the center of the culet of both the upper and lower diamonds to act as a pressure standard.[1] Benzoquinone was loaded into the gasket as a powder. It was loaded until there was no light passing through. The sample was hand tightened to ~3 GPa to ensure a seal. Raman spectroscopy data was taken before further compression. The DAC was compressed at a varying rate of 0.08-0.10 GPa min^{-1} until 47% of the maximum pressure was reached, 0.05-0.07 GPa min^{-1} until 71% of the maximum pressure was reached, 0.03-0.04 GPa min^{-1} until 86% of the maximum pressure was reached, and 0.01-0.02 GPa min^{-1}until maximum pressure was reached. Raman datawas taken every 2-3 GPa until maximum pressure was reached. Upon reaching maximum pressure, the DAC was decompressed at similar rates with a Raman scan taken at half the maximum pressure and again at 1-2 GPa.

A Renishaw inVia Raman spectrometer and microscope was used with a laser power of 1.34 mW and a 633 nm laser for *in situ* scans. To remove excess light a 5 μm pinhole was used. To get the laser to focus on samples through the diamonds, a long-pass 20x objective of 0.35 NA was used.

Synchrotron radiation was used for XRD data at the Advanced Photon Source (APS) at Argonne National Laboratory on the recovered sample. The 16-BM-D beamline created a 30 keV 5x5 μm beam with the MAR345 detector. The recovered sample has wide-angle reflections

of ±32º ω-scans with 10s/deg. of exposure in a 75 μm square area over three regions of the sample. The Dioptas software interpreted the resulting images to account for any shadows or absorptions of the diamond.[35]

IR data was obtained using a Bruker Hyperion 3000 Microscope. This resulted in a diffraction limited spatial resolution of three 10 μm spots in each gasket for samples in the gasket. After focusing on a sample, transmission spectra images were found with an MCT detector. The sample has ATR spectroscopy performed on it using a FTIR Bruker Vertex V70 possessing an ATR attachment sampling accessory.

Results

Kinetically controlled non-UV experiments with benzoquinone were performed to a maximum pressure of 12, 14, 16, 18, and 20 GPa. The rates for these different compressions were prescribed as detailed above in the methods section. For example, the 16 GPa sample was compressed at a rate of 0.08-0.10 GPa min^{-1} until it reached 7.62 GPa, 0.05-0.07 GPa min^{-1} until it reached 11.4 GPa, 0.03-0.04 GPa min^{-1} until it reached 13.7 GPa, and 0.01-0.02 GPa min^{-1}until it reached 16 GPa. When compressed slowly to 16 GPa, the recovered IR spectrum revealed that kinetic control can result in an sp^3 C-H peak observed 2920 cm^{-1} and O-H stretching from 3500-3150 cm^{-1} from recovered IR spectroscopy, but the XRD data revealed that an amorphous solid was made. Both can be found in Figure 3.3. The Raman spectrum yielded very similar results to fast compression but resulted in higher PL as observed in Figure 2.5. This is likely due to the added energy of UV light exciting the molecules and then the molecules relaxing via PL rather than fluorescence.

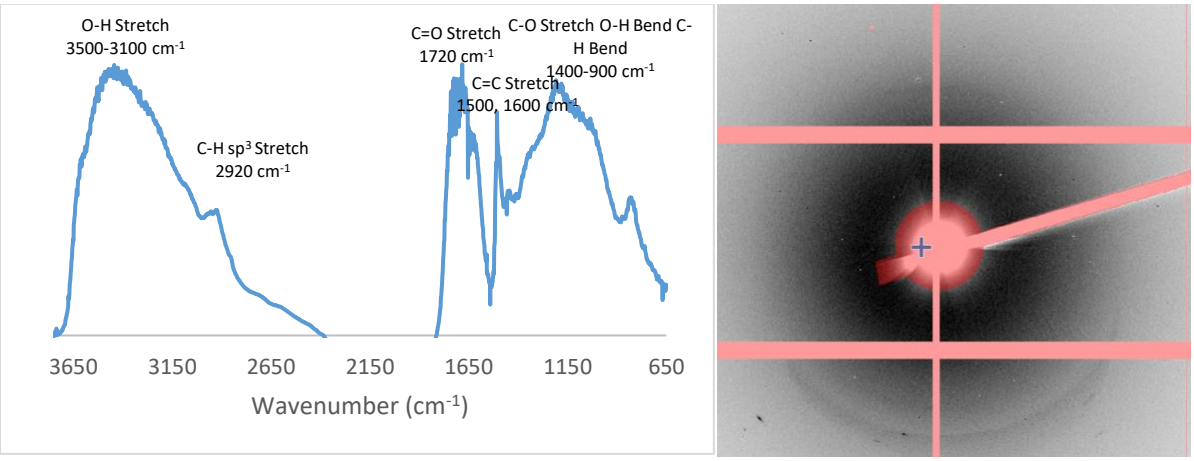

Figure 2.4. IR spectrum for 16 GPa slow compression showcasing an sp^3 peak at 2920 cm^{-1} (left) and XRD (right).

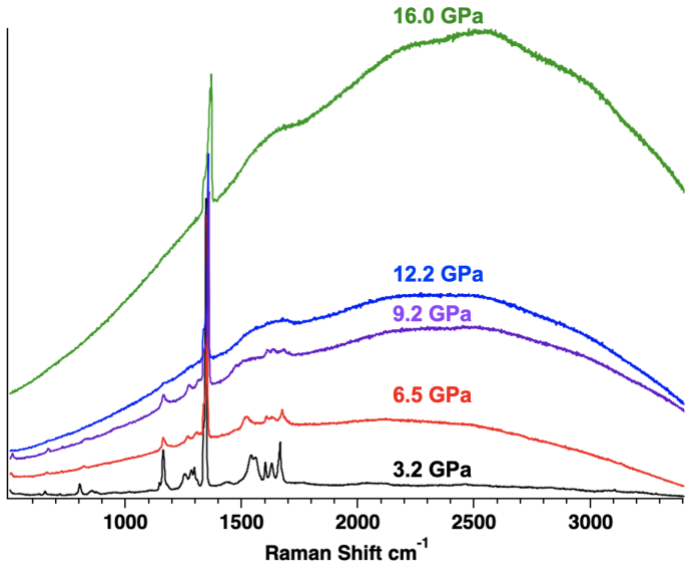

Figure 2.5. Raman data of slow compression to 16 GPa

These results were much more promising than any results received yet with the sp^3 peak, so the experiments were carried out to a maximum pressure of 12, 14, 18, & 20 GPa to see when possible nanothreads stopped forming and to see if the reaction gets altered in any way during these different maximum pressures. 14 GPa experiment resulted in a more intense diffraction pattern than observed previously in the 16 GPa experiment with similar results otherwise. The

sample was washed as well to remove any debris from the gasket to obtain a cleaner sample. Occasionally this can also wash away the sample or remove the diffraction ring, but ultimately resulted in a clean diffraction ring as shown below.

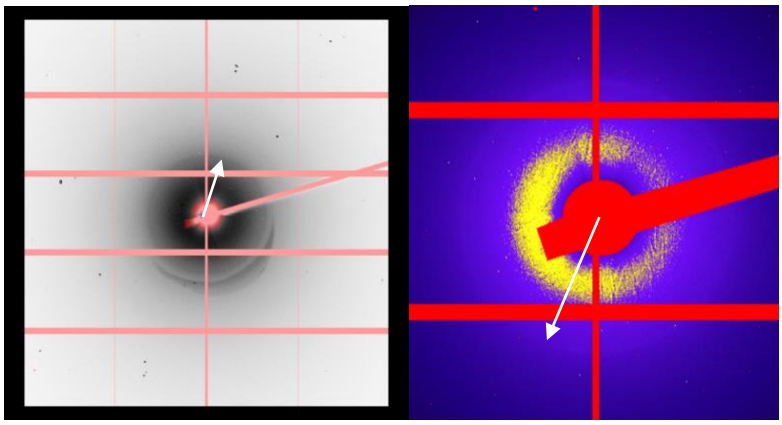

Figure 2.6. XRD of slow compression to 14 GPa before (left) and after washing (right). Diffraction observed at 5.3 Å.

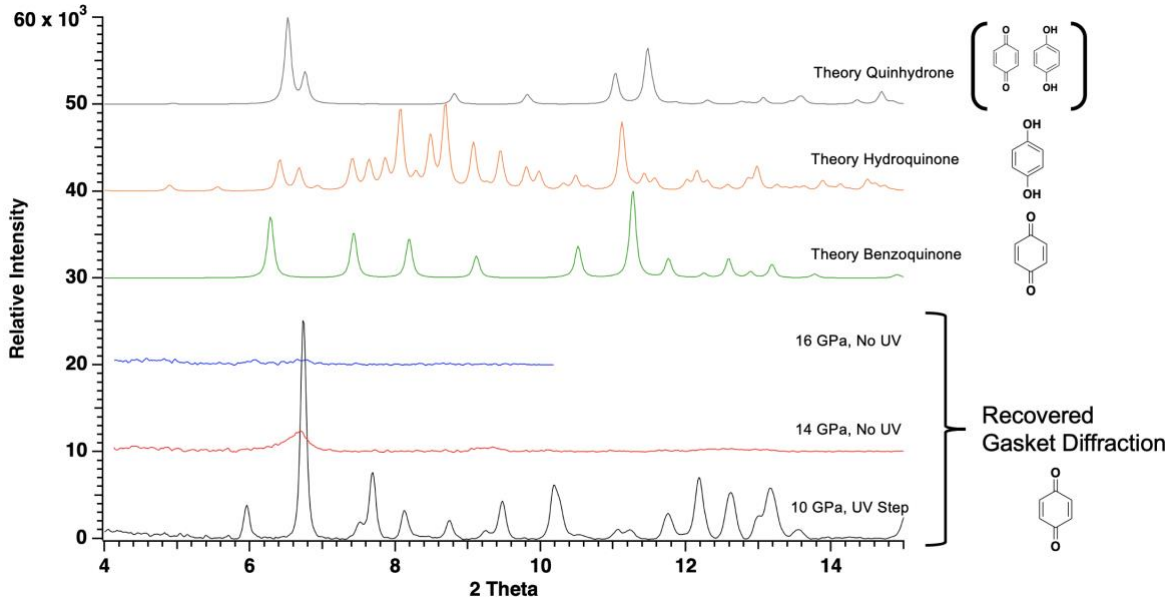

Figure 2.7. 2θ Graph of 14 GPa slow compression (red), 16 GPa slow compression (blue), and 10 GPa fast UV compression (lower black) of benzoquinone with computer modeled diffraction patterns for quinhydrone, hydroquinone, and benzoquinone.

When comparing 2θ graphs of both slow compression and the 10 GPa fast UV compression, there are far fewer peaks from small molecules in the kinetically controlled experiments, but a much weaker weak ring is obtained in the XRD data. Figure 2.7 compares the 14 and 16 GPa slow non-UV compressions to the 10 GPa fast UV compression. One can see the most intense diffraction ring is observed with the 10 GPa UV compression, but there are also many different peaks in this sample. This figure present theoretical powder XRD predictions for benzoquinone, hydroquinone, and the co-crystal of these molecules, quinhydrone generated from the Mercury software. These small molecules observed in the sample are not any hydroquinone, benzoquinone, or quinhydrone molecules as their modeled diffraction patterns do not align with the small molecules seen in the 10 GPa fast compression. This could be a result of side reactions due to UV exposure, or the fact that it is a fast compression. One such possibility is a semiquinone that could produce these various small molecules. Another possibility is benzoquinone being in a different phase than calculated. Further experimentation may produce XRD spectra with less side peaks compared to the fast UV compression when compressing slowly with UV exposure.

4. Slow UV Benzoquinone Compressions

Experimental Summary

A T301 stainless steel gasket was indented to approximately 12 GPa which achieved a width of 45-55 μm. After this an 80-167 μm hole was drilled with an electric discharge machine, and the gasket was placed into a symmetric Diamond Anvil Cell (DAC) equipped with 400 μm culet Type II diamonds. One ruby chip was placed at the center of the culet of both the upper and

lower diamonds to act as a pressure standard.[1] Benzoquinone was loaded into the gasket as a powder. It was loaded until there was no light passing through. The sample was hand tightened to ~1 GPa to ensure a seal. Raman spectroscopy was taken done further compression. The DAC was compressed at a varying rate of 0.08-0.10 GPa min^{-1} until 47% of the maximum pressure was reached, 0.05-0.07 GPa min^{-1} until 71% of the maximum pressure was reached, 0.03-0.04 GPa min^{-1} until 86% of the maximum pressure was reached, and 0.01-0.02 GPa min^{-1}until maximum pressure was reached. Raman data was taken every 2-3 GPa until maximum pressure was reached. Upon reaching maximum pressure, the DAC was decompressed at similar rates with a Raman scan taken at half the maximum pressure and again at 1-2 GPa.

A Renishaw inVia Raman spectrometer and microscope was used with a laser power of 1.34 mW and a 633 nm laser for *in situ* scans. To remove excess light a 5 μm pinhole was used. To get the laser to focus on samples through the diamonds, a long-pass 20x objective of 0.35 NA was used. UV radiation was projected through the top of this microscope with an output power of 96 mW, found using a Coherent PM3Q thermophile power sensor. The predicted power directed towards the sample is approximately 16 mW.[27]

Synchrotron radiation was used for XRD data at the Advanced Photon Source (APS) at Argonne National Laboratory on the recovered sample. The 16-BM-D beamline created a 30 keV 5x5 μm beam with the MAR345 detector. The recovered sample has wide-angle reflections of ±32º ω-scans with 10s/deg. of exposure in a 75 μm square area over three regions of the sample. The Dioptas software interpreted the resulting images to account for any shadows or absorptions of the diamond.[35]

IR data was obtained using a Bruker Hyperion 3000 Microscope. This resulted in a diffraction limited spatial resolution of three 10 μm spots in each gasket for samples in the

gasket. After focusing on a sample, transmission spectra images were found with an MCT detector. The sample has ATR spectroscopy performed on it using a FTIR Bruker Vertex V70 possessing an ATR attachment sampling accessory.

Results

Experiments were taken to a max pressure of 12, 14, 16, 18, and 20 GPa and yielded the most promising results of these methods to produce benzoquinone derived nanothreads. These pressure ranges were explored to determine when nanothreads started/stopped forming as well as to observe changes in reactivity with different maximum pressures. These samples had the same peaks as found previously with slow non-UV compressions but had much more intense diffraction patterns. The peaks are tabulated in Table 2.9. They show similar evidence of at least a partial isomerization into hydroquinone. They contain O-H stretching and C-O bends, but also had sp^3 C-H stretching peaks showing that it is likely nanothreads formed. Overlayed IR spectra for the 18 GPa slow non-UV and 14 slow UV compression can be found in Figure 2.9.

Regarding XRD, the strongest ring achieved for kinetically controlled UV experiments was achieved for the compression to 14 GPa as shown in Figure 2.8. This is the most intense signal received yet and diffracts at 5.3 Å just like previous experiments.

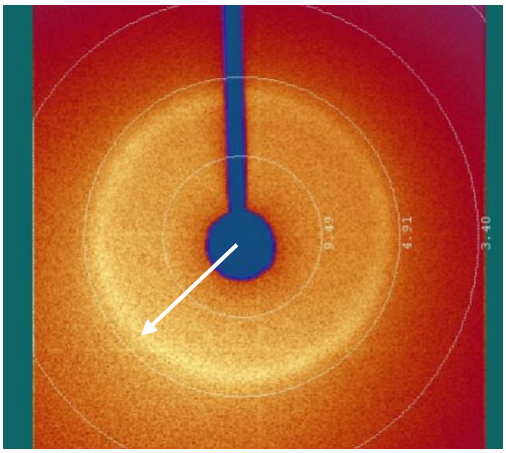

Figure 2.8. XRD from 14 GPa UV slow compression. Diffraction at 5.3 Å.

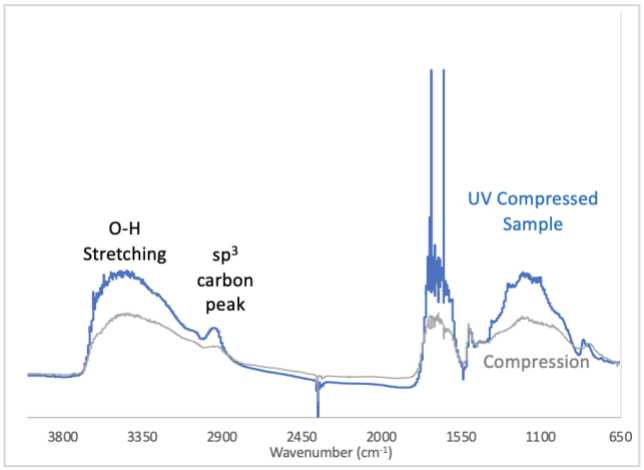

Figure 2.9. IR spectra of 18 GPa slow compression (grey) and the 14 GPa slow UV compression (blue)

Table 2.2. Tabulated IR peaks for benzoquinone, hydroquinone, and the recovered sample. Asterisk means that experimental region is very broad.

Peak Assignments	Benzoquinone Literature (cm^{-1}) [36]	Hydroquinone Literature (cm^{-1})[37]	Experimental (cm^{-1})
O-H Stretch	-	3256	3630
C-H sp^2	3058	3030	-
C-H sp^3	-	-	2920
C=O Stretch	1667	-	1720
C=C Aromatic*	1688	1460, 1470, 1478, 1517, 1610	1500, 1600
O-H Bend*	-	1355	1370
C-O*	-	1209	1290
C-H Bend*	1149	1192	1100
C=C Breathing	770	-	856

Found below is a summary of all previous experiments with benzoquinone. The fast compressions did not have many experiments run on them due to the believed viability of nanothreads in kinetically controlled reactions. Without UV light fast compressions only yielded amorphous products, but the addition of UV light made an intense diffraction ring showing crystallinity. An experiment of this nature was carried out to 18 GPa, but it has not been analyzed yet due to time constraints. The slow compressions with and without UV light all were carried out at 12, 14, 16, 18, and 20 GPa and all resulted in nanothreads except for the 16 GPa non-UV slow compression. The non-UV compressions had a much fainter diffraction ring than UV compressions. This leads one to believe that UV light acts as an initiator for nanothread formation.

Table 2.3. Summary table for benzoquinone reactions.

Method	10 GPa	12 GPa	14 GPa	16 GPa	18 GPa	20 GPa
Fast non-UV	-	-	-	Maybe, no IR could be obtained	-	-
Fast UV	Yes	-	-	-	?	-
Slow non-UV	-	Yes	Yes	No	Yes	Yes
Slow UV	-	Yes	Yes	Yes	Yes	Yes

Chapter 3

Compressions of Hydroquinone and Its Structural Isomers

1. Why Compress Benzoquinone Derivatives?

Benzoquinone exhibits several characteristics that can favor nanothread formation, including reduced aromaticity and intermolecular forces (H-bonding) that may guide a directional polymerization into a nanothread backbone. As discussed previously, benzoquinone is not an aromatic compound, but hydroquinone is, so benzoquinone should be more likely to compress at lower pressures.[21] Moreover, the isomerization from benzoquinone into hydroquinone has been reported under UV light,[27] so experiments in this chapter will detail the compression of hydroquinone to fully understand the reaction of benzoquinone. The alcohol groups will likely cause H-bonding directing the order and formation of nanothreads. Since the alcohol groups perfectly overlap one another, the hydrogen bonding could go along with the axis of the thread.

Likewise, catechol, which contains ortho substituted alcohol groups, and resorcinol, which contains meta substituted alcohol groups, have follow some of the same properties as hydroquinone, from the aromaticity to the possibility of directional ordering in possible nanothread formation. These molecules could also have ulterior reaction pressures compared to benzoquinone and hydroquinone, which could make these more viable as nanothread precursors, but this is not as likely because their crystal structures are less favorable. The crystal structures don’t line up as nicely as benzoquinone and hydroquinone.

These molecules also help to explain the reasons behind reaction of benzoquinone to produce nanothreads. We can learn from them by seeing what peaks are present or absent in the recovered products. If nanothreads can be formed from resorcinol and catechol, then we can also try to predict in which ways these molecules initiate their polymerizations. This can help lead us to discovering how benzoquinone nanothreads are formed.

One can see how these closely related derivatives will provide additional information. They can help test what properties of benzoquinone help aid in reaction. Additionally, it helps set the stage for what might be happening during *in situ* isomerization by testing to see if this isomerization acts as an initiator. The aromaticity found in these compounds may affect which pressure they react at and could possibly help us understand if the lack of aromaticity helps benzoquinone form nanothreads. These molecules can also demonstrate if there is order to nanothreads being formed with the *in situ* isomerization or if the UV light simply acts as the initiator.

2. Compression of Catechol

Experimental Summary

A T301 stainless steel gasket was indented to approximately 12 GPa which achieved a width of 45-55 μm. After this a 100 μm hole was drilled with an electric discharge machine, and the gasket was placed into a symmetric Diamond Anvil Cell (DAC) equipped with 400 μm culet Type II diamonds. One ruby chip was placed at the center of the culet of both the upper and lower diamonds to act as a pressure standard.[1] Catechol was loaded into the gasket as a powder. It was loaded until there was no light passing through. The sample was hand tightened to ~3 GPa

to ensure a seal. Raman spectroscopy was taken before further compression. The DAC was compressed at a rate of ~9 GPa/hour stepwise with Raman data taken in between until maximum PL was obtained via Raman spectroscopy. Upon reaching maximum pressure, the DAC was rapidly decompressed to half the maximum pressure and at 1-2 GPa with an associated Raman scan.

A Renishaw inVia Raman spectrometer and microscope was used with a laser power of 1.34 mW and a 633 nm laser for *in situ* scans. To remove excess light a 5 μm pinhole was used. To get the laser to focus on samples through the diamonds, a long-pass 20x objective of 0.35 NA was used.

The sample was also analyzed by an Olympus BX62 microscope that contained a 20x objective and a blue-field correction plate. To achieve more easily viewed colors to the eye, a 535 nm half wave-plate was used to enhance the polarization.

Synchrotron radiation was used for XRD at the Advanced Photon Source (APS) at Argonne National Laboratory on the recovered sample. The 16-BM-D beamline created a 30 keV 5x5 μm beam with the MAR345 detector. The recovered sample has wide-angle reflections of ±32º ω-scans with 10s/deg. of exposure in a 75 μm square area over three regions of the sample. The Dioptas software interpreted the resulting images to account for any shadows or absorptions of the diamond.[35]

IR was obtained using a Bruker Hyperion 3000 Microscope. This resulted in a diffraction limited spatial resolution of three 10 μm spots in each gasket for samples in the gasket. After focusing on a sample, transmission spectra images were found with an MCT detector. The sample has ATR spectroscopy performed on it using a FTIR Bruker Vertex V70 possessing an ATR attachment sampling accessory.

Results

Catechol was explored to determine when PL begins and ends and see if this could be a possible reaction pressure. This experiment will also allow comparison to benzoquinone and its other derivatives, resorcinol and hydroquinone. Due to this there was no target pressure other than finding where maximum PL was achieved. This fast compression ended at 19.24 GPa due the complete disappearance of peaks, particularly the sp^2 stretch at 3100 cm^{-1}. Raman scans were taken sequentially around every 3-4 GPa. Raman data was compiled and shown in Figure 3.1 with peak assignments done in Table 3.1 for the first Raman scan. This is done to confirm that the initial load only contained Catechol and not something else. All the peaks line up or can be explained otherwise, ruby or diamond, so the sample is indeed Catechol. The peak around 3100 cm^{-1} representing sp^2 C-H stretching is diminished as pressure continues to increase with the development of a shoulder closer to 3000 cm^{-1} before being overshadowed by PL when it starts at 7.18 GPa until it is completely succumbed at 16.47 GPa.

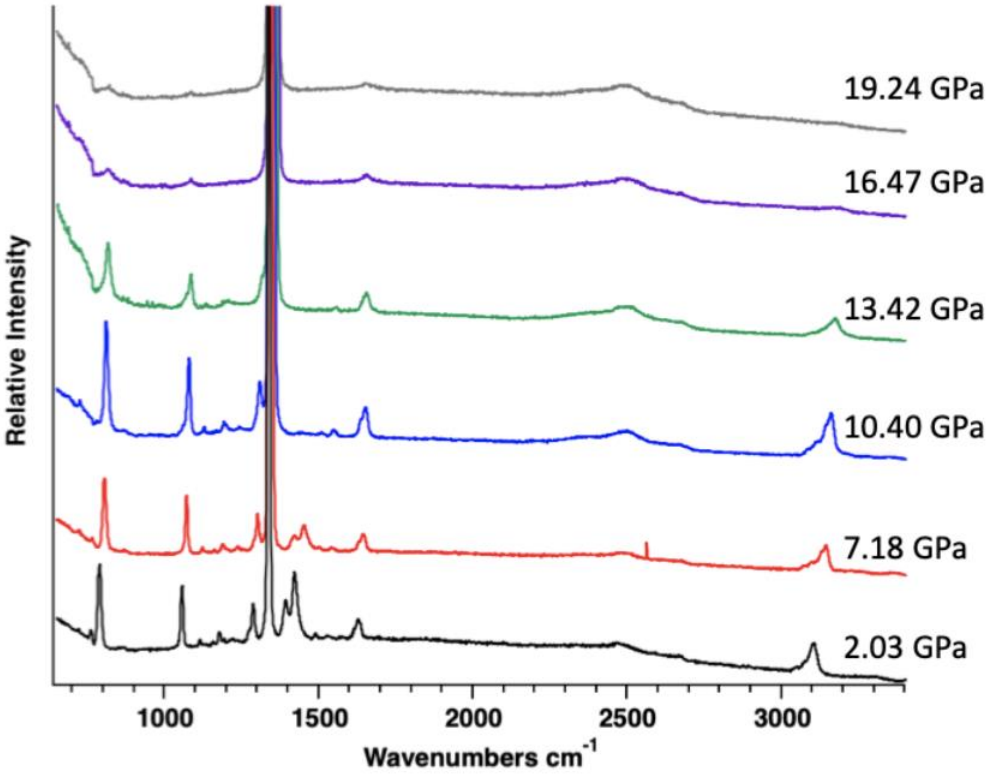

Figure 3.1. *In situ* Raman spectrum for fast compression of catechol to 19 GPa

Table 3.1. Peak assignments for catechol compression.

Peak Assignments	Literature (cm^{-1})[38]	Experimental (cm^{-1})
O-H Stretching	3324, 3458	3300
C-H sp^2	3045-3070	3104
C=C Aromatic	1476, 1515, 1606, 1614	1480, 1525, 1628
Ruby Interference	-	1392, 1423
Diamond Interference	-	1350
C-O	1255, 1276	1287
O-H	1181	1177
C-H	1042, 1104, 1163	1056, 1114
Lattice Modes	204, 213, 296, 564, 582, 719, 775	761, 788

This compression also had microscope images taken after compression which were polarized to reveal if there was any crystallinity to the sample. This image can be found below in Figure 3.2. The magenta color reveals that there is no crystallinity in the center. To the side of this space the molecule takes on orange and brown colors indicating that there are solids obviously present. This typically means that there is an amorphous solid which XRD confirmed since it showed no diffraction ring.

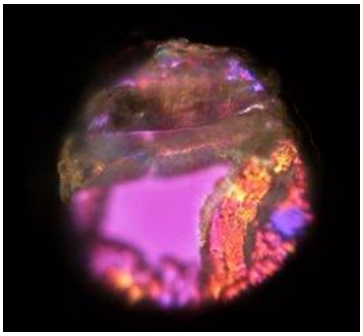

Figure 3.2. Polarized light image of recovered sample from catechol compression.

To make any conclusions about the possible formation of catechol nanothreads, further experimentation and analysis must be done. This ultimately would mean completing a slow compression, slow UV compression, and fast UV compression with catechol and determining the best reaction methods for nanothread formation. Ideally more analysis should be done on the most promising candidates beyond XRD and IR data, including *in situ* XRD and x-ray electron spectroscopy (XPS). These additional tests will help reveal crystallinity after compression in XRD, any sp^3 C-H stretches are shown better in IR, *in situ* XRD could reveal a well ordered 6-fold diffraction pattern consistent with a nanothread, and XPS will help give ratios of each atom which could help to reveal how the molecule is structured and if it underwent any changes.

3. Compression of Resorcinol

Experimental Summary

A T301 stainless steel gasket was indented to approximately 12 GPa which achieved a width of 45-55 μm. After this a 100 μm hole was drilled with an electric discharge machine, and the gasket was placed into a symmetric Diamond Anvil Cell (DAC) equipped with 400 μm culet Type II diamonds. One ruby chip was placed at the center of the culet of both the upper and lower diamonds to act as a pressure standard.[1] Catechol was loaded into the gasket as a powder. It was loaded until there was no light passing through. The sample was hand tightened to ~3 GPa to ensure a seal. Raman spectroscopy was taken before further compression. The DAC was compressed at a rate of ~9 GPa/hour stepwise with Raman taken in between until maximum PL was obtained via Raman. Upon reaching maximum pressure, the DAC was rapidly decompressed to half the maximum pressure and at 1-2 GPa with an associated Raman scan.

A Renishaw inVia Raman spectrometer and microscope was used with a laser power of 1.34 mW and a 633 nm laser for *in situ* scans. To remove excess light a 5 μm pinhole was used. To get the laser to focus on samples through the diamonds, a long-pass 20x objective of 0.35 NA was used.

The sample was also analyzed by an Olympus BX62 microscope that contained a 20x objective and a blue-field correction plate. To achieve more easily viewed colors to the eye, a 535 nm half wave-plate was used to enhance the polarization.

Synchrotron radiation was used for XRD data at the Advanced Photon Source (APS) at Argonne National Laboratory on the recovered sample. The 16-BM-D beamline created a 30 keV 5x5 μm beam with the MAR345 detector. The recovered sample has wide-angle reflections of ±32° ω-scans with 10s/deg. of exposure in a 75 μm square area over three regions of the sample. The Dioptas software interpreted the resulting images to account for any shadows or absorptions of the diamond.[35]

IR data was obtained using a Bruker Hyperion 3000 Microscope. This resulted in a diffraction limited spatial resolution of three 10 μm spots in each gasket for samples in the gasket. After focusing on a sample, transmission spectra images were found with an MCT detector. The sample has ATR spectroscopy performed on it using a FTIR Bruker Vertex V70 possessing an ATR attachment sampling accessory.

Results

Like catechol, resorcinol was only initially explored while trying to determine a maximum PL. These studies were utilized just like previously for catechol as it would help to identify when PL begins and ends as well as a possible reaction pressure. Resorcinol is a very similar molecule to catechol, but could have altered nanothread structure due to the location of

the alcohol groups on the two molecules. This molecule is not as likely to form nanothreads due to a longer centroid:centroid distance of 5.7 Å as well as a slipped crystal structure. The pressure at which max PL was achieved was at 25.83 GPa as at this point the Raman began to become very wavy, and no discernable peaks could be observed. Resorcinol's Raman scan can be found in Figure 3.3 with an accompanying peak table. Any peaks present have been overtaken by PL at 16.78 GPa. There is a spike around 2900 cm^{-1} shown with an asterisk, representing a cosmic ray. These cosmic rays can occasionally appear in Raman scattering when a star bursting in outer space results in a wave hitting the detector during the scan.[3] Other than this the Raman looks very similar to that of catechol, besides not having a shoulder appear to the left of the sp^2 peak.

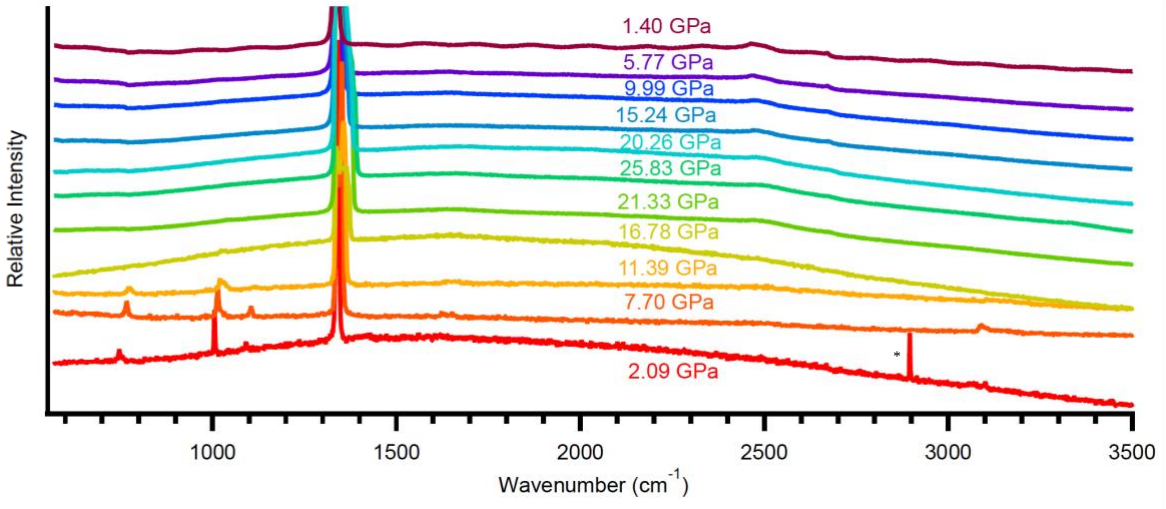

Figure 3.3. *In situ* Raman spectrum for the compression of Resorcinol to 25.83 GPa. The asterisk defines a cosmic ray.

Table 3.2. Peak assignments for resorcinol compression.

Peak Assignments	Literature (cm^{-1})[39]	Experimental (cm^{-1})
O-H	-	-
C-H sp^3	-	3089
C=C Aromatic	1608	1623
Diamond	-	1350
C-H	1085	1100
C=C	1000	1014
Lattice Modes	734, 744	767

Resorcinol also had polarized light images taken of it resulting in Figure 3.4. On the left hand side an orange color is observed showing that it is partially solid but lacks crystallinity. Over towards the right-hand side a wide array of colors can be observed which typically represents a crystalline solid, but sadly XRD data showed that it was amorphous.

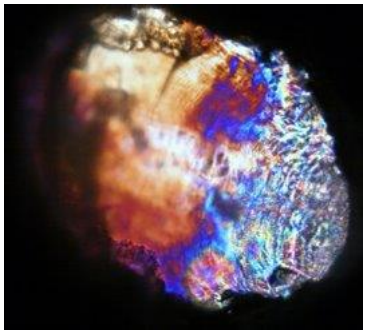

Figure 3.4. Polarized light image for sample collected from resorcinol compression.

Like catechol, any solid conclusions about the possible formation of resorcinol nanothreads, require further experimentation and analysis. The three other types of compressions – fast UV, slow, and slow UV must be completed as these could cause resorcinol to react

differently. These are not likely to form nanothreads, but need a full set of experiments. This different reaction could help lead to the production of nanothreads. Like catechol, XRD, *in situ* XRD, IR, and XPS should be conducted. These additional tests will give us the same information that was discussed previously in the conclusion of the catechol experiments.

4. Compression of Hydroquinone

Experimental Summary

A T301 stainless steel gasket was indented to approximately 12 GPa which achieved a width of 45-55 μm. After this a 100 μm hole was drilled with an electric discharge machine, and the gasket was placed into a symmetric Diamond Anvil Cell (DAC) equipped with 400 μm culet Type II diamonds. One ruby chip was placed at the center of the culet of both the upper and lower diamonds to act as a pressure standard.[1] Hydroquinone was loaded into the gasket as a powder. It was loaded until there was no light passing through. The sample was hand tightened to ~3 GPa to ensure a seal. Raman spectroscopy was done before further compression. The DAC was compressed at a rate of ~9 GPa/hour stepwise with Raman taken in between until maximum PL was obtained via Raman. Upon reaching maximum pressure, the DAC was rapidly decompressed to half the maximum pressure and at 1-2 GPa with an associated Raman scan.

A Renishaw inVia Raman spectrometer and microscope was used with a laser power of 1.34 mW and a 633 nm laser for *in situ* scans. To remove excess light a 5 μm pinhole was used. To get the laser to focus on samples through the diamonds, a long-pass 20x objective of 0.35 NA was used.

Synchrotron radiation was used for XRD data at the Advanced Photon Source (APS) at Argonne National Laboratory on the recovered sample. The 16-BM-D beamline created a 30 keV 5x5 μm beam with the MAR345 detector. The recovered sample has wide-angle reflections of ±32° ω-scans with 10s/deg. of exposure in a 75 μm square area over three regions of the sample. The Dioptas software interpreted the resulting images to account for any shadows or absorptions of the diamond.[35]

IR data was obtained using a Bruker Hyperion 3000 Microscope. This resulted in a diffraction limited spatial resolution of three 10 μm spots in each gasket for samples in the gasket. After focusing on a sample, transmission spectra images were found with an MCT detector. The sample has ATR spectroscopy performed on it using a FTIR Bruker Vertex V70 possessing an ATR attachment sampling accessory.

Results

The following experiment was performed in collaboration with Morgan Dierolf to complete the family of disubstituted -OH groups. Hydroquinone was compressed once as a fast compression to 17 GPa that was halted prematurely due to gasket expansion. Pictures of this expansion can be found in Figure 3.5 where it expanded to be approximately 2-3 times the original volume. The fast non-UV experiment yielded the best results. The Raman data shows a very strong initial sp^2 peak, peaks around 1600 cm^{-1} due to aromatic C=C bonds, and a strong peak around 800 cm^{-1} related to the C-O bond. PL begins at about 9.87 GPa and continues to increase until 16.69 GPa when the compression was halted prematurely due to gasket expansion. At 16.69 GPa, it is also important to note that a shoulder appears to the left of the original sp^2 peak as a series of two humps. It is a very wide peak and could be the sp^2 peak dissipating with the increased PL, but it could also be a sp^3 peak. The Raman data can be seen in Figure 3.6.

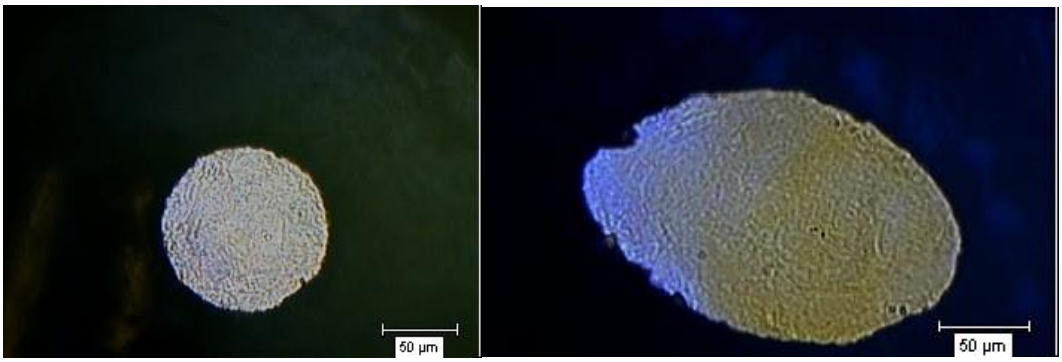

Figure 3.5. Original gasket size around 4.60 GPa (left) and expanded gasket at 16.69 GPa.

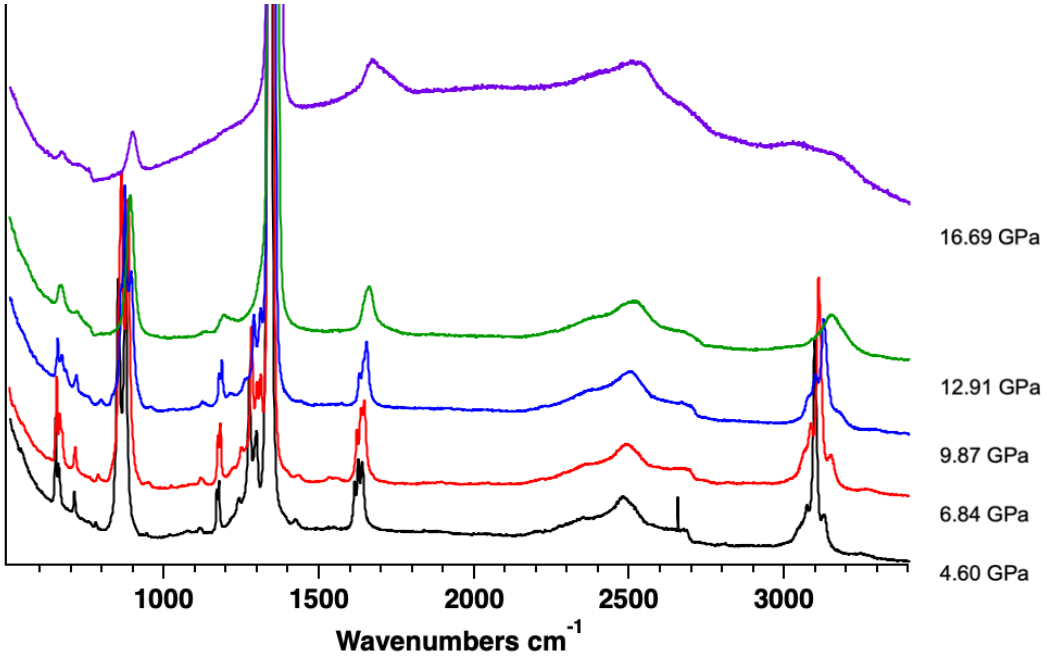

Figure 3.6. Raman spectrum for fast compression of hydroquinone to 17 GPa.

When the hydroquinone sample was subjected to XRD, it revealed the sample was amorphous. IR spectroscopy was explored as this method of analysis allows one to see sp^3 C-H stretches and O-H stretches much easier than by using Raman data, and it ended up revealing the most about the sample. Within the IR spectrum, O-H stretching at ~3400 cm^{-1}, C-O stretching at 1210 and 1097 cm^{-1}, and C=C stretching at 1512 and 1470 cm^{-1} are all present which could indicate either precursor or nanothread formation. Irregardless these IR stretches show that one

of these two species exist. The most important features in the IR spectrum were a sp^3 peak around 2960 cm^{-1} and C=O stretching peak at 1708 cm^{-1}. The sp^3 peak shows that nanothreads could be present, but the C=O stretch shows that a tautomerization may have occurred to some extent form a keto-enol tautomer.[26] This means that a pathway with ketone groups could be more favorable than one with alcohols, and the reaction energy may be lower. The IR spectra can be found in Figure 3.7.

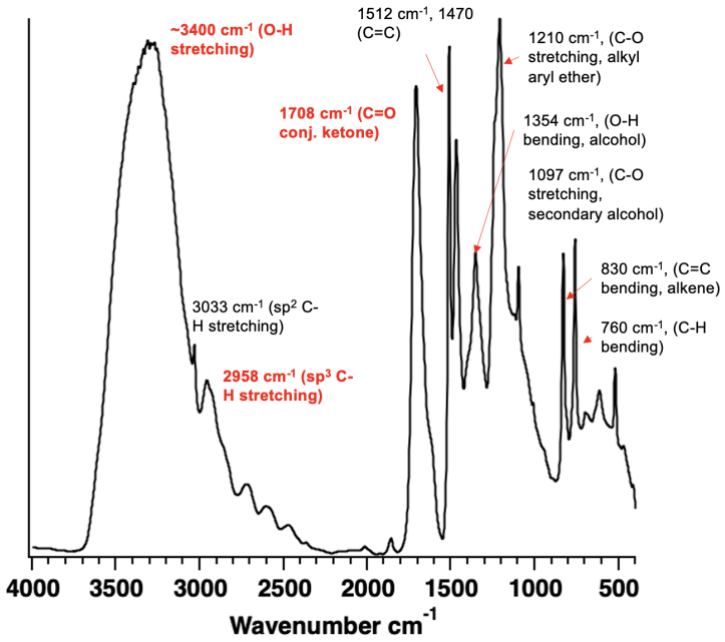

Figure 3.7. IR spectra for fast compression of hydroquinone to 17 GPa.

Table 3.3. Peak assignments for hydroquinone spectra.

Peak Assignments	Raman Literature (cm^{-1})[37]	Raman Experimental (cm^{-1})	IR Literature (cm^{-1})[37]	IR Experimental (cm^{-1}) (Post Compression)
O-H Stretch	3216	-	3256	3400
C-H sp^2	3029, 3067, 3080	3073, 3098, 3129	3030	3033
C-H sp^3	-	-	-	2958
C=O Stretch	-	-	-	1708
C=C Aromatic	1408, 1601, 1608, 1625	1428, 1614, 1626, 1630	1460, 1470, 1478, 1517, 1610	1470, 1512
O-H Bend	1370	-	1355	1354
Diamond	-	1350	-	-
C-O	1252, 1254, 1257	1274, 1298	1209	1097, 1210
C-H Bend	1163, 1169	1177	-	760
C=C Bend	855	852, 876	-	830
Lattice Modes	650, 704	651, 711	-	-

In the future hydroquinone should be compressed further with UV light and in slow compressions. The results for hydroquinone are consistent with nanothread formation except for the XRD data. This experiment was stopped prematurely, so it should be carried out again to see if a crystalline structure can form at higher pressures. Nonetheless hydroquinone undergoes a keto-enol tautomerization which must be energetically favorable at high-pressure, so this could mean ketone groups are necessary for nanothread formation particularly in the case of benzoquinone.

Chapter 4

Conclusion and Future Work

1. Conclusions

Resorcinol, catechol, and hydroquinone are all closely related molecules to benzoquinone, and all bring different properties to the table which may favor nanothread formation. The former two need to be explored more heavily to see if other methods bring about different results, and the current experiments must be analyzed further to determine if they are not to producing nanothreads. The Raman scans for these molecules don't nanothread formation.

Hydroquinone has a volume dependent change that creates a large barrier to produce potential nanothreads. More experimentation is required with varying pressures and other methods to see if the proposed initiator to benzoquinone is required for their formation. It would be reasonable to postulate that hydroquinone does in fact form carbon nanothreads; this is supported by the IR spectrum gathered from the recovered sample.

Benzoquinone gives the most promising results. The fast compression did not give promising results, but when UV light is added at maximum pressure an intense diffraction ring appears in the XRD data. It also has many other peaks that are likely from small molecules. Another sample has been compressed in this manner to 6 GPa higher, but the sample was not yet be analyzed via XRD and IR to see if these small molecules disappear.

By far benzoquinone's most promising compressions were kinetically controlled with and without UV exposure. The non-UV samples exhibited a very weak diffraction ring that can be associated with nanothreads in tandem with the IR showing an sp^3 peak. Unlike the fast

compressions, there are no small molecules present, so this method could be a "cleaner" path to nanothread production. Slow compressions with UV exposure yielded the most intense XRD diffraction rings of any other compression and contained much more intense peaks for sp^3 carbons via IR. This method also yielded much more intense alcohol peaks compared to the non-UV compressions revealing that isomerization is happening *in situ*. The presence of the alcohol could indicate that the benzoquinone and hydroquinone molecules must adhere to one another to initiate this polymerization. This can continue down the line to extend the carbon network without further need of the other molecule.

On top of all the experiments outlined above XPS should be conducted as it would be extremely beneficial to compare the ratio of hydrogens, carbons, and oxygens. This comparison could help reveal how much benzoquinone and hydroquinone are present to tell more about this initiator step. Beyond this not much more physical analysis can be done, but theoretical studies should be done as well to confirm the identity of these recovered samples. Confirmation of nanothread products can be done by comparing theoretical and physical results.

2. Future Work

In the future there should be theoretical studies on the most promising nanothread products. These will help to confirm the identity of what product was recovered and possibly even reveal what the benzoquinone to hydroquinone ratio is. Additionally, more experiments should be conducted on resorcinol and catechol to determine if they react differently with UV light exposure or with kinetically controlled experiments. These molecules should not be ruled out completely until these experiments can be conducted.

In addition to this, the isomerization of benzoquinone into hydroquinone appeared to help this molecule form products, so this pathway should be explored more. For future experimentation more molecules with reduced aromaticity and ability to isomerize should be compressed. This method could be used in tandem with other prior techniques which have been identified to help in the compression of carbon nanothreads.

BIBLIOGRAPHY

[1]Hayashi, T.; Ahm Kim, Y.; Natsuki, T.; Endo, M. Mechanical Properties of Carbon Nanomaterials. *ChemPhysChem* **2007**, *8*, 999 – 1004

[2]Dai, L.; Chang, D.; Baek, J.-B.; Lu, W. Carbon Nanomaterials for Advanced Energy Conversion and Storage. *Small* **2012**, *8 (8)*, 1130–1166.

[3] Iijima, S. Helical Microtubules of Graphitic Carbon. *Nature* **1991**, *354*, 56–58.

[4]Fitzgibbons, T. Synthesis of Carbon Materials via the Cold Compression of Aromatic Molecules and Carbon Nanostructures. Ph.D. Dissertation, The Pennsylvania State University, University Park, PA, 2014.

[5]Biswas, A. Mechanochemical Pathways Towards Heteroatom-Doped Carbon Nanothreads. Ph.D. Dissertation, The Pennsylvania State University, University Park, PA, 2021.

[6]Chen, B.; Hoffmann, R.; Cammi, R. The Effect of Pressure on Organic Reactions in Fluids—a New Theoretical Perspective. *Angew. Chem., Int. Ed.* **2017**, *56* (37), 11126–11142.

[7]Fitzgibbons, T. C.; Guthrie, M.; Xu, E.; Crespi, V. H.; Davidowski, S. K.; Cody, G. D.; Alem, N.; Badding, J. V. Benzene-Derived Carbon Nanothreads. *Nat. Mater.* **2014**, *14* (1), 43–47.

[8]Ciabini, L.; Santoro, M.; Bini, R.; Schettino, V. High pressure reactivity of solid benzene probed by infrared spectroscopy. *Chem. Phys.* **2002**, *116*, 2928-2935.

[9]Schettino, V.; Bini, R. Constraining molecules at the closest approach: chemistry at high pressure. *Chem. Soc. Rev.* **2007**, *36*, 869-880.

[10]Citroni, M.; Bini, R.; Foggi, P.; Schettino, V. Role of excited electronic states in the high-pressure amorphization of benzene. *Proc. Natl. Acad. Sci.* **2008**, *105*, 7658-7663.

[11]Clark, A. *Fountains of Paradise*; Harcourt Brace Jovanovich, 1979

[12]Stojkovic, D.; Zhang, P.; Crespi, V. H. Smallest Nanotube: Breaking the Symmetry of sp^3 Bonds in Tubular Geometries. *Phys. Rev. Lett.* **2001**, *87* (12), 125502-1-125502-1.

[13]Wen, X.-D.; Hoffmann, R.; Ashcroft, N. W. Benzene under High Pressure: A Story of Molecular Crystals Transforming to Saturated Networks, with a Possible Intermediate Metallic Phase. *J. Am. Chem. Soc.* **2011**, *133* (23), 9023–9035.

[14]Zhan, H.; Zhang, G.; Bell, J. M.; Tan, V. B.; Gu, Y. High Density Mechanical Energy Storage with Carbon Nanothread Bundle. *Nat. Comm.* **2020**, *11* (1).

[15]Li, X.; Baldini, M.; Wang, T.; Chen, B.; Xu, E.; Vermilyea, B.; Crespi, V. H.; Hoffmann, R.; Molaison, J. J.; Tulk, C. A.; Guthrie, M.; Sinogeikin, S.; Badding, J. V. Mechanochemical Synthesis of Carbon Nanothread Single Crystals. *J. Am. Chem. Soc,* **2017**, *139* (45), 16343–16349.

[16]Xu, E.; Lammert, P. E.; Crespi, V. H. Systematic Enumeration of sp^3 Nanothreads. *Nano Lett.* **2015**, *15* (8), 5124–5130.

[17]Duan, P.; Li, X.; Wang, T.; Chen, B.; Juhl, S. J.; Koeplinger, D.; Crespi, V. H.; Badding, J. V.; Schmidt-Rohr, K. The Chemical Structure of Carbon Nanothreads Analyzed by Advanced Solid-State NMR. *J. Am. Chem. Soc.* **2018**, *140* (24), 7658–7666.

[18]Li, X.; Wang, T.; Duan, P.; Baldini, M.; Huang, H.-T.; Chen, B.; Juhl, S. J.; Koeplinger, D.; Crespi, V. H.; Schmidt-Rohr, K.; Hoffmann, R.; Alem, N.; Guthrie, M.; Zhang, X.; Badding, J. V. Carbon Nitride Nanothread Crystals Derived from Pyridine. *J. Am. Chem. Soc.* **2018**, *140* (15), 4969–4972.

[19]Biswas, A.; Ward, M. D.; Wang, T.; Zhu, L.; Huang, H.-T.; Badding, J. V.; Crespi, V. H.; Strobel, T. A. Evidence for Orientational Order in Nanothreads Derived from Thiophene. *J. Phys. Chem. Lett.* **2019**, *10* (22), 7164–7171.

[20]Huang, H.-T.; Zhu, L.; Ward, M. D.; Wang, T.; Chen, B.; Chaloux, B. L.; Wang, Q.; Biswas, A.; Gray, J. L.; Kuei, B.; Cody, G. D.; Epshteyn, A.; Crespi, V. H.; Badding, J. V.; Strobel, T. A. Nanoarchitecture through Strained Molecules: Cubane-Derived Scaffolds and the Smallest Carbon Nanothreads. *J. Am. Chem. Soc.* **2020**, *142* (42), 17944–17955.

[21]Huss, S.; Wu, S.; Chen, B.; Wang, T.; Gerthoffer, M.; Hoffmann, R.; Crespi, V.; Badding, J.; Elacqua, E. Scalable Synthesis of Crystalline One-Dimensional Carbon Nanothreads through Modest-Pressure Polymerization of Furan. *ACS Nano* **2021**, *15*, 4134–4143.

[22]Ward, M. D.; Tang, W. S.; Zhu, L.; Popov, D.; Cody, G. D.; Strobel, T. A. Controlled Single-Crystalline Polymerization of $C_{10}H_8 \cdot C_{10}F_8$ Under Pressure. *Macromolecules* **2019**, *52* (20), 7557–7563.

[23]Wang, Y.; Dong, X.; Tang, X.; Zheng, H.; Li, K.; Lin, X.; Fang, L.; Sun, G.; Chen, X.; Xie, L.; Bull, C. L.; Funnell, N. P.; Hattori, T.; Sano-Furukawa, A.; Chen, J.; Hensley, D. K.; Cody, G. D.; Ren, Y.; Lee, H. H.; Mao, H. Pressure-Induced Diels-Alder Reactions in C_6H_6-C_6F_6 Cocrystal towards Graphane Structure. *Angew. Chem., Int. Ed.* **2019**, *58* (5), 1468–1473.

[24]Tang, W. S.; Strobel, T. A. Evidence for Functionalized Carbon Nanothreads from π-Stacked, *Para*-Disubstituted Benzenes. *J. Phys. Chem. C* **2020**, *124* (45), 25062–25070.

[25]Gerthoffer, M. C.; Wu, S.; Chen, B.; Wang, T.; Huss, S.; Oburn, S. M.; Crespi, V. H.; Badding, J. V.; Elacqua, E. ‘Sacrificial’ Supramolecular Assembly and Pressure-Induced

Polymerization: Toward Sequence-Defined Functionalized Nanothreads. *Chem. Sci.* **2020**, *11* (42), 11419–11424.

[26]Gerthoffer, M. C.; Xu, B.; Wu, S.; Cox, J.; Huss, S.; Oburn, S. M.; Lopez, S. A.; Crespi, V. H.; Badding, J. V.; Elacqua, E. Mechanistic Insights into the Pressure-Induced Polymerization of Aryl/Perfluoroaryl Co-Crystals. *Polym. Chem.* **2022**, *13* (10), 1359–1368.

[27]Oburn, S. M.; Huss, S.; Cox, J.; Gerthoffer, M. C.; Wu, S.; Biswas, A.; Murphy, M.; Crespi, V. H.; Badding, J. V.; Lopez, S. A.; Elacqua, E. Photochemically Mediated Polymerization of Molecular Furan and Pyridine: Synthesis of Nanothreads at Reduced Pressures. *J. Am. Chem. Soc.* **2022**, *144* (48), 22026–22034.

[28]Badding, J. V. High-Pressure Synthesis, Characterization, and Tuning of Solid State Materials. *Annu. Rev. Mater. Sci.* **1998**, *28* (1), 631–658.

[29]Yang, X.; Wang, X.; Wang, Y.; Li, K.; Zheng, H. From Molecules to Carbon Materials—High Pressure Induced Polymerization and Bonding Mechanisms of Unsaturated Compounds. *Crystals* **2019**, *9* (10), 490–511.

[30]Mao, H. K.; Xu, J.; Bell, P. M. Calibration of the Ruby Pressure Gauge to 800 Kbar under Quasi-Hydrostatic Conditions. *J. Geophys. Res.* **1986**, *91* (B5), 4673.

[31]Ciabini, L.; Santoro, M.; Gorelli, F. A.; Bini, R.; Schettino, V.; Raugei, S. Triggering dynamics of the high-pressure benzene amorphization. *Nat. Mater.* **2007**, *6*, 39-43.

[32]Kikuchi, S. A History of the Structural Theory of Benzene - the Aromatic Sextet Rule and Huckel's Rule. *J. Chem. Ed.* **1997**, *74* (2), 194.

[33]Kettle, A. J.; Winterbourn, C. C. Oxidation of Hydroquinone by Myeloperoxidase. Mechanism of Stimulation by Benzoquinone. *J. Biol. Chem.* **1992**, *267* (12), 8319–8324.

[34]Andersen, F. A.; Bergfeld, W. F.; Belsito, D. V.; Hill, R. A.; Klaassen, C. D.; Liebler, D. C.; Marks, J. G.; Shank, R. C.; Slaga, T. J.; Snyder, P. W. Final Amended Safety Assessment of Hydroquinone as Used in Cosmetics. *Int. J. Toxicol.* **2010**, *29*, 274S-287S.

[35]Spackman, M.A.; Jayatilaka, D. CrystEngComm, 2009, 11, 19-32

[36]Becker, E. D.; Charney, E.; Anno, T. Molecular Vibrations of Quinones. Vi. A Vibrational Assignment for *p*-Benzoquinone and Six Isotopic Derivatives. Thermodynamic Functions of *p*-Benzoquinone. *J. Chem. Phys.* **1965**, *42* (3), 942–949.

[37]Kubinyi, M. J.; Keresztury, G. Infrared and Raman Spectra of Hydroquinone Crystalline Modifications. In *Progress in Fourier Transform Spectroscopy*, Budapest, Hungary, Aug 27-Sep 1; 1995; Mink, J.; Keresztury, G.; Kellner, R; Springer: Vienna, 1997; 525–528. https://link.springer.com (accessed March 13th, 2023)

[38]Greaves, S. J.; Griffith, W. P. Vibrational Spectra of Catechol, Catechol-D2 and -D6 and the Catecholate Monoanion. *Spectrochim. Acta, Part A* **1991**, *47* (1), 133–140.

[39]Tripathi, G. N. Crystal Spectra and Vibrational Assignments in α-Resorcinol. *J. Chem. Phys.* **1981**, *74* (1), 250–255.

ACADEMIC VITA

Robert Connor Burns

814-569-3008 | rcb5497@psu.edu

EDUCATION

The Pennsylvania State University
Bachelor of Science in Chemistry
Schreyer Honors College — Expected Graduation: May 2023

CUSTOMER SERVICE EXPERIENCE

Penn State Admissions, **Tour Guide Evaluations Intern** — Aug 2022 – Present

- Managed all campus tour evaluations to assess tour quality for over 200 tour guides
- Determined which Welcome Desk Assistant will evaluate 1-2 tour guides for 5 tours each week
- Corresponded with prospective students about campus visits using a central inbox of a CRM platform

Penn State Lion Scouts

Tour Director — Apr 2022 – Present

- Oversaw training of 70 new tour guides for the largest touring organization at Penn State over 6 weeks, simultaneously organizing guest speakers, shadowing, and mock tour opportunities
- Introduced additional inclusive language trainings to promote campus tour inclusiveness
- Staffed new events added throughout the semester with tour guides to ensure more intimate tour groups

Tour Guide — Oct 2020 – Present

- Guided tour groups of 10-50 prospective students and families during a 90-minute walking tour

Penn State Admissions, **Welcome Desk Assistant** — Aug 2021 – Aug 2022

- Facilitated 5-6 campus tours per week or special events with check-in and tour assignments
- Supported visitation team with undergraduate admissions events of up to 3,000 guests

UPMC Altoona, **Hospital Host** — May 2021 – Aug 2021

- Tended to inpatients while taking their orders and served daily meals
- Edited food tickets to ensure they complied with inpatient's diet

Marzoni's, **Host/Server/Bartender** — Sep 2017 – Dec 2021

- Seated customers, took food orders, served food, and made drinks
- Communicated with departments across the restaurant to deliver meals timely and accurately
- Checked other bartender/servers nightly work before they were allowed to leave

SCIENCE-BASED WORK EXPERIENCE

Department of Chemistry Elacqua Group, **Undergraduate Research Assistant** — Oct 2021 – Present

- Exposed sp^2 carbon containing molecules at high pressures up to 20 GPa to different conditions to alter reactivity and form carbon nanothreads at lower pressures
- Created a poster for American Chemical Society
- Writing and presenting an honors thesis for university and faculty approval

Penn State Health Promotion and Wellness, **Healthworks Volunteer** — Aug 2021 – Dec 2022

- Presented 50-minute talks on health related topics regarding sleep, nutrition, sexual health, and stress management at first-year seminars and club meetings

- Promoted different health and wellness opportunities available on campus via tabling

AWARDS

- Dean's List 7/7 Semesters
- Benjamin Bear & Alice Keller Scholarship 2021 – 2023
- Benkovic Summer Research Award Recipient 2022
- Han-Silverman Open Doors Scholarship 2021 – 2022
- A. Martarano Open Doors Scholarship 2021 – 2022